Molecular Oncology

FEBS PRESS science publishing by scientists

Recurrent cancer-associated ERBB4 mutations are transforming and confer resistance to targeted therapies

Veera K. Ojala[1,2,3], Sini Ahonen[1], Sara Peltola[1,2,3,4], Aura Tuohisto-Kokko[1], Olaya Esparta[1], Peppi Suominen[1], Anne Jokilammi[1,2], Iman Farahani[1,2,3,4], Deepankar Chakroborty[1,2,3], Nikol Dibus[1], Steffen Boettcher[5], Tomi T. Airenne[6,7], Mark S. Johnson[6,7], Lisa D. Eli[8], Klaus Elenius[1,2,4,9] and Kari J. Kurppa[1,2]

1 Institute of Biomedicine, and MediCity Research Laboratory, University of Turku, Finland
2 Turku Bioscience Centre, University of Turku and Åbo Akademi University, Finland
3 Turku Doctoral Programme of Molecular Medicine, Finland
4 InFLAMES Research Flagship, University of Turku, Finland
5 Department of Medical Oncology and Hematology, University of Zurich and University Hospital Zurich, Switzerland
6 Structural Bioinformatics Laboratory, Biochemistry, Faculty of Science and Engineering, Åbo Akademi University, Turku, Finland
7 InFLAMES Research Flagship Center, Åbo Akademi University, Turku, Finland
8 Translational Medicine and Diagnostics, Puma Biotechnology Inc., Los Angeles, CA, USA
9 Department of Oncology, Turku University Hospital, Finland

Keywords
activating mutations; cancer; drug resistance; ERBB4; HER4; oncogene

Correspondence
K. J. Kurppa and K. Elenius, MediCity Research Laboratory, University of Turku, Tykistökatu 6A, Turku 20520, Finland
E-mail: kjkurp@utu.fi; klaele@utu.fi

Klaus Elenius and Kari J. Kurppa contributed equally to this article.

(Received 4 July 2025, revised 10 November 2025, accepted 10 December 2025)

doi:10.1002/1878-0261.70189

Receptor tyrosine kinase ERBB4 (HER4) is frequently mutated in human cancer, and *ERBB4* mutations have been identified in patients relapsing on targeted therapy. Here, we addressed the functional consequences of recurrent cancer-associated *ERBB4* mutations that are located at regions important for receptor activation and/or are paralogous to known oncogenic hotspot mutations in other *ERBB* genes. Eleven out of 18 analyzed mutations were transforming in cell models, thus suggesting oncogenic potential for more than half of the recurrent ERBB4 mutations. More detailed analyses of the most potent mutations, S303F, E452K, and L798R, showed that they are activating, can co-operate with other ERBB receptors and are sensitive to clinically available second-generation pan-ERBB inhibitors neratinib, afatinib, and dacomitinib. Furthermore, the S303F mutation, together with a previously identified activating ERBB4 mutation, E715K, promoted resistance to third-generation EGFR inhibitor osimertinib in EGFR-mutant lung cancer model *in vitro* and *in vivo*. Together, these results are expected to facilitate clinical interpretation of the most recurrent cancer-associated *ERBB4* mutations. The findings provide rationale for testing the efficacy of clinically used pan-ERBB inhibitors in patients harboring driver *ERBB4* mutations both in the treatment-naïve setting, and upon development of resistance to targeted agents.

1. Introduction

All four members of the epidermal growth factor receptor (EGFR)/ERBB/HER family of receptor tyrosine kinases (RTK) are frequently mutated or amplified in cancer [1,2]. Numerous ERBB-targeted

Abbreviations
EGF, epidermal growth factor; NRG-1, neuregulin-1; NSCLC, non-small-cell lung cancer; RTK, receptor tyrosine kinase; TKI, tyrosine kinase inhibitor; UMAP, uniform manifold approximation and projection.

therapies have been developed but their currently approved indications include only cancers with *EGFR* or *ERBB2* alterations. Of these, the second-generation irreversible ERBB tyrosine kinase inhibitors (TKI) neratinib, afatinib and dacomitinib, are termed pan-ERBB inhibitors as they potently inhibit EGFR, ERBB2 and ERBB4, although not directly the kinase-impaired ERBB3 [3]. Yet, despite the high frequency of *ERBB4* missense mutations in various cancer types (up to 30% in nonmelanoma skin cancer, Fig. S1A,B) and characterization of several potentially oncogenic *ERBB4* mutations [4–8], the rationale for clinically targeting ERBB4 in cancer has not been fully developed. The reasons for this include the perplexing results of the role of ERBB4 in cancer as well as the rarity of the distinct *ERBB4* mutations that have been characterized as oncogenic thus far.

ERBB4 mutations have also been found in patients who developed resistance to EGFR-targeted therapies [9–12], warranting further investigation into the potential role of *ERBB4* mutations in therapy resistance. In addition, activation of ERBB4 signaling has been associated with EGFR- and ERBB2-targeted therapy resistance in multiple studies [9,13–17], raising the possibility that mutant ERBB4 could be a potential therapeutic target to combat resistance to targeted therapies.

Unlike other ERBB receptors, ERBB4 has four different isoforms that have partly different, even opposing functions, and both tumor-suppressive and oncogenic functions have been described for ERBB4 [18–22]. Importantly, the oncogenic functions have been attributed to the ERBB4 isoforms that are predominant in cancer tissues and/or whose relative expression compared to the other isoforms is increased in cancer [23–25].

Another challenge in studying ERBB4 in cancer has been to choose which of the hundreds of different cancer-associated *ERBB4* mutations to select for functional analysis to identify potential oncogenic drivers, since *ERBB4* does not have clear mutational hotspots that would suggest functional relevance. Thus far, the strategies to characterize activating *ERBB4* mutations have included (a) selecting mutations found in a specific cancer type, including melanoma and lung cancer [4,7], (b) an unbiased functional screen of nearly all theoretically possible *ERBB4* missense mutations [6], and (c) selecting *ERBB4* mutations found from cancer cell lines that are sensitive to ERBB-targeting drugs [26]. Although several activating gain-of-function *ERBB4* mutations have indeed been identified and many of these mutants have also been shown to be sensitive to pan-ERBB inhibitors, the rarity of these specific variants in patients makes it difficult to clinically assess their predictive value for ERBB4-targeted therapy.

The immensely increased body of tumor sequencing data over the past 10 years has, however, resulted in the emergence of specific recurrent *ERBB4* mutations in hotspot-like regions of the *ERBB4* gene. Additionally, the rare but transforming *ERBB4* mutations structurally characterized thus far [6,7] act via stabilizing dimerization interfaces similar to many of the known oncogenic hotspot mutations of ERBB2 and ERBB3 [27,28]. To better facilitate the evaluation of the predictive potential of the cancer-associated *ERBB4* mutations, we functionally characterized 18 of the recurrent *ERBB4* variants. We show that majority (11/18) of the *ERBB4* mutations have significant transforming potential and that the most potent mutants are biochemically activating and co-operate with other ERBB receptors—most strikingly S303F. We also demonstrate for the first time that the activating *ERBB4* mutations are able to promote resistance to EGFR-targeted therapy in the context of EGFR-mutant non-small-cell lung cancer (NSCLC). Importantly, our data indicate that recurrent *ERBB4* gain-of-function mutations are sensitive to clinically used second-generation pan-ERBB inhibitors.

2. Materials and methods

2.1. Cell culture

Phoenix-AMPHO (RRID: CVCL_H716; a gift from Dr Garry Nolan), Ba/F3 (RRID: CVCL_0161; DSMZ ACC 300), PC-9 (RRID: CVCL_B260; a gift from Dr Pasi Jänne), and T47D (RRID: CVCL_0553; ATCC HTB-133) cells were cultured in RPMI 1640 (EuroClone, Pero, Italy, Gibco, Billings, MT, USA or Lonza, Basel, Switzerland), MCF10a cells (RRID: CVCL_0598; ATCC CRL-10317) in DMEM/F-12 (Lonza), and HEK293T (RRID: CVCL_1926; ATCC CRL-11268), COS7 (RRID: CVCL_0224; ATCC CRL-1651), and MCF7 cells (RRID: CVCL_0031; ATCC HTB-22) cells in DMEM (EuroClone, Gibco or Lonza). All media were supplemented with 10% FCS (Biowest, Bradenton, FL, USA), 50 $U \cdot mL^{-1}$ penicillin and streptomycin solution (Gibco or Lonza) and 2 mM L-glutamine (Gibco or Lonza). Ba/F3 cell medium was additionally supplemented with 5% WEHI cell-conditioned medium as a source of IL3 while the media for IL3-independent Ba/F3 cells were supplemented or not with neuregulin-1β (NRG-1) (396-HB-050; R&D Systems, McKinley Place NE, MN, USA). MCF10a cell medium was additionally supplemented with 20 $ng \cdot mL^{-1}$ EGF (AF-100-15; Peprotech, Cranbury, NJ, USA), 0.5 $\mu g \cdot mL^{-1}$ hydrocortisone (H-0888; Sigma, St. Louis, MO, USA), 100 $ng \cdot mL^{-1}$ cholera toxin (C-

8052; Sigma), and 10 μg·mL^{-1} insulin (I9278; Sigma). T47D and MCF7 cells were supplemented with 10 μg·mL^{-1} human insulin (I9278; Sigma). Cells were routinely tested for mycoplasma infection using MycoAlert (Lonza) and experiments were performed with mycoplasma-free cells. All cell lines used were either purchased from vendors (DSMZ, ATCC) or authenticated within 3 years of performed experiments. Cell line authentication was performed as a service at the University of Helsinki from 30 μg of DNA, using the GenePrint 24 system (Promega, Madison, WI, USA).

2.2. Plasmids

The following previously described retroviral mammalian expression plasmids were used: *pBABE-puro-gateway-eGFP* [6], *pBABE-puro-gateway-EGFR* [29], *pBABE-puro-gateway-ERBB2* [26], *pBABE-puro-gateway-ERBB3* [26], *pBABE-puro-gateway-ERBB4JM-aCYT-2* [6], *pcDNA3.1neo(−)-ERBB4JM-aCYT-2* [22], *pMLDg/pRRE*, *pMD2.G*, and *pRSV-Rev* (gifts from Dr Didier Trono; Addgene plasmids #12251, #12259, and #12253) [30]. Expression constructs encoding ERBB4 JM-a CYT-2 point mutants listed in Table S1 were created by cloning mutant inserts from *pDONR221*-vectors (Genscript) into *pBABE-puro-gateway* retroviral mammalian expression vector (a gift from Matthew Meyerson; Addgene plasmid #51070; http://n2t.net/addgene:51070; RRID:Addgene_51070) [27] using LR clonase II mix (Invitrogen, Waltham, MA, USA) for the LR Gateway recombination reaction. All generated constructs were verified by sequencing the insert.

2.3. Generation of cell lines with stable ERBB4 expression

For retroviral transductions, Phoenix-AMPHO packaging cells were transfected with retroviral *pBABE-puro-gateway* constructs encoding ERBB4 variants or enhanced green fluorescent protein (eGFP) (vector control) using FuGENE 6 transfection reagent (Promega) according to manufacturer's protocol. The retroviral supernatants of Phoenix-AMPHO cells were harvested 24 and 48 h after transfection and used immediately to infect Ba/F3, MCF10a, or PC-9 cells. Cell pools with stable expression were selected with 2 μg·mL^{-1} puromycin (Gibco) for 48 h and then maintained in 1 μg·mL^{-1} puromycin.

2.4. Ba/F3 cell transformation assay

Ba/F3 cells stably expressing *ERBB4* variants or vector control were washed twice with PBS to deplete IL3 and 1×10^6 cells were seeded in 10 mL IL3-free culture medium (10% serum) supplemented or not with 20 ng·mL^{-1} NRG-1 or with IL3 (5% WEHI cell-conditioned medium) as a control. Cell viability was measured from Day 0 up to saturation density with the MTT assay (CellTiter 96 nonradioactive cell proliferation assay; Promega) by collecting 100 μL of the cell suspension into 96-well plate wells in quadruplicates. The doubling times were calculated using the equation $\text{doubling time} = \frac{\ln(2)}{\text{growth rate}}$, and $\text{growth rate} = \frac{\ln\left(\frac{N_t}{N_0}\right)}{t}$, where, t is the time in hours reaching saturation density, N_t is absorbance at saturation density, and N_0 is the absorbance at seeding density. The doubling times for cells growing in 20 ng·mL^{-1} NRG-1 were normalized to the average of wild-type ERBB4 of each independent experiment. Kruskal–Wallis test was used for statistical testing and false discovery rate was controlled by two-stage linear step-up method of Benjamini, Krieger, and Yekutieli, considering $q < 0.05$ as significant. GRAPHPAD PRISM 10 was used to perform statistical analyses and creating the dot plots.

2.5. MCF10a cell transformation assay

MCF10a cells stably expressing ERBB4 variants or vector control were seeded at 2000 cells per well density into 96-well plate wells in triplicates in the presence of EGF. Next day, EGF-free medium (10% serum) supplemented or not with 50 ng·mL^{-1} NRG-1 was changed and cell viability was measured with the MTT assay on Days 0 and 8 of EGF deprivation. Day 8 cell viability fold changes to Day 0 were calculated and normalized to the average of wild-type ERBB4 of each independent experiment. Kruskal–Wallis test was used for statistical testing and false discovery rate was controlled by two-stage linear step-up method of Benjamini, Krieger, and Yekutieli, considering $q < 0.05$ as significant. GRAPHPAD PRISM 10 was used to perform statistical analyses and creating the dot plots.

2.6. Structural analysis

The S303F mutation was analyzed using the crystal structure PDB: 2AHX (2.4 Å resolution [31]) for the tethered conformation and PDB: 3U7U (3.03 Å [32]) for the active conformation. The E452K mutation was analyzed using PDB: 3U7U, the extracellular structure of an active ERBB4 dimer with bound NRG-1. The L798R mutation was analyzed using PDB: 3BCE, the intracellular structure of an active ERBB4 asymmetric kinase dimer and PDB: 3BBT, the inactive form with bound active site inhibitor lapatinib [33]. The

mutant rotamers were selected using the inbuilt tool of PYMOL (The PyMOL Molecular Graphics System, Version 2.4, Schrödinger, LLC., New York, NY, USA).

2.7. Western blotting

Cells were lysed in lysis buffer containing 1% Triton X-100, 10 mM Tris-Cl, pH 7.4, 150 mM NaCl, 1 mM EDTA, 10 mM NaF and supplemented with Halt Protease and Phosphatase Inhibitor Cocktail (Thermo Scientific, Waltham, MA, USA). Equal amounts of proteins were separated by SDS/PAGE, transferred to nitrocellulose membranes and analyzed using the following primary antibodies: anti-phospho-EGFR Tyr1086 (#2220), anti-EGFR (#2232, Cell Signaling Technology, Danvers, MA, USA), anti-phospho-ERBB2 Tyr1248 (#2247; Cell Signaling Technology), anti-ERBB2 (MA5-14057; Invitrogen), anti-phospho-ERBB3 Tyr1289 (#4791; Cell Signaling Technology), anti-ERBB3 (#12708, Cell Signaling Technology), anti-phospho-ERBB4 antibodies: Tyr984 (#3790, Cell Signaling Technology), Tyr1162 (PAB0486, Abnova, Taipei City, Taiwan) and Tyr1284 (#4757, Cell Signaling Technology), anti-ERBB4 (clone E200, ab32375, Abcam), anti-phospho-AKT Ser473 (#4060; Cell Signaling Technology), anti-AKT (#2920; Cell Signaling Technology), anti-phospho-ERK Thr202/Tyr204 (#9101; Cell Signaling Technology), anti-ERK (#9102; Cell Signaling Technology), anti-phospho-STAT5 Tyr694 (#9351; Cell Signaling Technology), anti-STAT5a (sc-271542, Santa Cruz, Dallas, TX, USA), and anti-β-actin (A5441; Sigma Aldrich). Signals were detected using Odyssey CLx imaging system (LI-COR) and densitometric quantifications were performed with the IMAGE STUDIO LITE v5.2 software.

2.8. Lentiviral-mediated *Erbb3* knockdown in Ba/F3 cell lines

Doxycycline-inducible murine *Erbb3* shRNA (shErbb3; TRCN0000023432) expression construct was generated by ligating oligonucleotides listed in Table S1 into *Tet-pLKO-neo* vector (a gift from Dmitri Wiederschain: Addgene plasmid #21916; http://n2t.net/addgene:21916; RRID:Addgene_21916) [34]. The construct was verified by sequencing the insert.

For lentiviral shRNA transduction, HEK293T packaging cells were transfected with lentiviral packaging plasmids (pMLDg/pRRE, pMD2.G, and pRSV-Rev) and *Tet-pLKO-neo-shErbb3* and viral supernatants were used to infect Ba/F3 cells. Stable cell pools were selected with 500 $\mu g \cdot mL^{-1}$ neomycin (Geneticin, Gibco) for 5 days and then maintained in 250 $\mu g \cdot mL^{-1}$ neomycin. Ba/F3 EGFR L790M and L858R mutant cell lines were generated in our previous study [29].

To study the effect of *Erbb3* knockdown on ERBB4-mediated Ba/F3 cell transformation, cells expressing doxycycline-inducible *Erbb3* shRNA construct were subjected to the transformation assay described in chapter 2.4 in the presence or absence of 800 $ng \cdot mL^{-1}$ doxycycline (Millipore, Burlington, MA, USA). Pairwise comparisons between doubling times of the transformed cells cultured in the presence or absence of doxycycline were made with Welch two-sample t test. P-values were corrected for multiple comparisons by Bonferroni method and $P < 0.0001$ was considered significant.

2.9. Dimerization assays

To analyze ERBB4 homodimerization, COS7 cells were seeded on 6-well plates and transiently transfected with FuGENE 6 and 1 μg of the *pBABE-puro-gateway* constructs encoding wild-type or mutant ERBB4 or vector control. Next day, serum-free medium supplemented or not with 50 $ng \cdot mL^{-1}$ NRG-1 was changed after washing the cells with PBS. After 4-day serum starvation, cells were washed three times with ice-cold PBS and treated with 2 mM membrane impermeable BS_3 crosslinker (Thermo Fisher) in PBS for 1 h on ice. The reaction was quenched with ice-cold 50 mM Tris–HCl, pH 7.4, 150 mM NaCl for 15 min on ice, after which the cells were washed three times with ice-cold PBS and lysed. The protein samples were run on 6% SDS/PAGE gels and ERBB4 dimers were analyzed by western blotting.

To analyze ERBB4 heterodimerization, COS7 cells were seeded on 10-cm dishes and transiently cotransfected with FuGENE 6 and 3 μg + 3 μg of the *pBABE-puro-gateway* constructs encoding ERBB4 variants or vector control with either EGFR, ERBB2, or ERBB3. Cells were serum-starved for 4 days in the presence or absence of 50 $ng \cdot mL^{-1}$ NRG-1 as described above and lysed. Lysates containing 500 μg protein were precleared with 20 μL protein G Sepharose beads (Cytiva, Marlborough, MA, USA) for 2 h at +4 °C and subjected to immunoprecipitation by overnight incubation with either anti-ERBB4 (HFR-1 or E200), anti-EGFR, anti-ERBB2, or anti-ERBB3 antibodies and subsequent 2-h incubation with 20 μL protein G Sepharose beads. Beads were washed four times with 1 mL lysis buffer and boiled in SDS/PAGE loading buffer. Co-immunoprecipitating ERBB receptors were analyzed by western blotting.

2.10. Neratinib efficacy in patients with an ERBB4 alteration

Neratinib efficacy data, cancer types, and co-alterations of patients harboring an *ERBB4* alteration,

enrolled in PUMA-NER-5201, the SUMMIT trial (NCT01953926), and treated with neratinib as a single agent (240 mg·day^{-1}) were obtained from Puma Biotechnology, Los Angeles, CA, USA (for patients enrolled based on an *ERBB4* mutation—previously unpublished data) and cBioPortal (for patients with *ERBB4* as a co-altered gene, enrolled based on an *ERBB2* or *ERBB3* mutation).

2.11. Patient data

For the analysis of gene alteration frequencies, cancer type, and co-occurring alterations in ERBB4-mutant cancer patients, clinical cancer sample data were obtained from cBioPortal (https://cbioportal.org) [35–37], AACR GENIE (https://genie.cbioportal.org) [38], COSMIC (https://cancer.sanger.ac.uk/cosmic) [39] in January 2024.

2.12. Drug sensitivity assays

IL3-independent Ba/F3 cells (20 000 cells per well) expressing ERBB4 variants were plated in 96-well plates in IL3-free medium (10% serum) containing or not 10 ng·mL^{-1} NRG-1 and vector control cells were plated in medium containing IL3 (10% serum). The cells were incubated in the presence of 0.00067–2.5 μM of neratinib (Puma Biotechnology), afatinib (Boehringer Ingelheim am Rhein, Germany), dacomitinib (Cayman Chemicals, Ann Arbor, MI, USA) or DMSO only for 72 h before measuring cell viability of quadruplicate samples with MTT assay (as described above). For PC-9 cells expressing ERBB4 variants, 3000 cells per well were plated on 96-well plates. The next day, the growth medium was changed to a medium supplemented or not with 50 ng·mL^{-1} NRG-1, and the cells were treated with 0.002–2.5 μM osimertinib (SelleckChem, Houston, TX, USA) or DMSO in triplicate. Cell viability was measured with MTT assay after 72-h incubation. The drugs and DMSO were dispensed with D300 Digital Dispenser (HP). GRAPHPAD PRISM 10 was used to fit dose–response curves with the variable slope equation and least squares regression and plotted by indicating mean ± standard deviation. For Ba/F3 experiments, the IC50 values were extrapolated from the fitted curves and normalized to that of wild-type ERBB4 of each independent experiment. For statistical analysis, normalized IC50 values of 2–3 independent experiments were analyzed by one-sample *t* test, adjusting the *P*-values for multiple comparisons by the Bonferroni method and considering $P < 0.05$ as significant.

2.13. Long-term drug treatment assays

PC-9 cells expressing ERBB4 variants were plated on 12-well plates (25 000 cells per well). The following day, the growth medium was changed to a medium (10% serum) supplemented or not with 50 ng·mL^{-1} NRG-1, and the cells were treated with 100 nM osimertinib (SelleckChem) or DMSO in triplicate. Medium was changed every 5 days. After 14-day incubation, the cells were washed with PBS, fixed with methanol (10 min), and stained with 0.5% crystal violet. After 15-min incubation, the wells were washed three times with 2 mL of PBS, followed by one wash with 2 mL of ultrapure water (Milli-Q). After washes, the wells were allowed to air dry. The stained cells were imaged using an Epson scanner, and the scanned images of three independent experiments were quantified in IMAGEJ, using the ColonyArea plugin [40]. One-way ANOVA was used to assess statistical significance, using Šídák's multiple comparisons test.

2.14. Mouse xenograft experiments

Seven-week-old female Rj:NMRI-Foxn1$^{nu/nu}$ mice were purchased from Janvier Labs and were allowed to acclimate for at least 6 days prior to the initiation of the experiment at Turku Center for Disease Modeling (TCDM). Mice were housed under a controlled environment (12-h light cycle, temperature 21 ± 3°C, humidity 55% ± 15%, specific pathogen-free) at the Central Animal Laboratory of the University of Turku. Chow and tap water were available *ad libitum*. Xenografts were established by subcutaneous injections of PC-9 cells expressing ERBB4 variants (5×10^6 cells in 50% Matrigel matrix (#354234, BD Biosciences, San Jose, CA, USA)) in the right flank of each mouse. Tumor growth was monitored one to three times a week by bilateral caliper measurements and the tumor volume was calculated using the formula $V = 0.5 \times \text{length} \times \text{width}^2$. Tumors were allowed to reach 250 ± 50 mm^3 in size on average before randomization into vehicle or osimertinib treatment groups ($n > 4$–5 or $n > 11$–13 mice per group, respectively). Powdered osimertinib (HY-15772, MedChemExpress, Monmouth Junction, NJ, USA) was added to normal chow mixture (V1554, ssniff Spezialdiäten) and pelleted by ssniff Spezialdiäten. The prepared chow containing 35 mg·kg^{-1} osimertinib or not (vehicle) was fed to mice, and after 189 days, osimertinib treatment was withdrawn by changing the mice to receive normal chow. Mice were sacrificed at indicated time points according to our protocol approved by the Regional State Administrative of Southwestern Finland (license

number: ESAVI/7740/2023). Animals were monitored daily and mice having welfare problems were sacrificed before the intended end point of the study. The animal study was carried out according to the regulations of the Finnish Act on Animal Experimentation (62/2006).

Tumor growth curves of individual mice and Kaplan–Meier curves of relapse-free survival were plotted with GRAPHPAD PRISM 10. Log rank test was used to compare the relapse-free survival of osimertinib-treated mice with tumors expressing either mutant or wild-type ERBB4.

2.15. Single-cell RNA-sequencing analysis

Single-cell RNA-sequencing data from PC-9 xenografts treated with vehicle or osimertinib [41] was downloaded from GEO (accession number GSE131604). CELLRANGER (version 7.1.0) aggregate analysis was performed on count data using default parameters to normalize count data by sequencing depth. The expression of ERBB4 ligands *NRG1*, *NRG2*, *NRG3*, *NRG4*, *HBEGF*, *EREG*, and *BTC* was analyzed using LOUPE BROWSER (version 8).

3. Results

3.1. Selection of recurrent *ERBB4* mutations for functional characterization

To search for potentially actionable *ERBB4* mutations among the most recurrent cancer-associated *ERBB4* mutations, we conducted an *in silico* analysis of the curated set of nonredundant studies ($n = 217$) included in the cBioPortal, consisting of 70 655 patient samples from 147 cancer types (Fig. S1A). *ERBB4* was altered in 3.5% of the analyzed samples in which missense mutations were the most common *ERBB4* alteration (87% of *ERBB4* altered samples) (Fig. 1A). The analysis identified 2117 somatic *ERBB4* missense mutations of which 182 (9%) were annotated as putative drivers in cBioPortal based on OncoKB curated evidence [42,43] (Fig. 1A). *ERBB4* missense mutations were found to be most frequent in skin cancers (30% in nonmelanoma, 14% in melanoma) and least frequent in embryonal (0.2%) cancers (Fig. S1B).

While the missense mutations were distributed across the 1308 amino acid sequence of ERBB4, lacking obvious hotspot mutations such as observed for example in EGFR or KRAS, clusters of recurrent mutations could be identified (Fig. 1B). These clusters tended to be located in specific regions that are targeted by activating mutations in other oncogenic ERBB family members [27,28,44–46] and/or are important for receptor activation [31,32,47], suggesting functional relevance (red boxes in Fig. 1B). Some recurrent mutations were located in the unstructured C-terminal tail of ERBB4 (Fig. 1B). We selected in total 18 *ERBB4* missense mutations (indicated in Fig. 1B) that were recurrent and/or located in the abovementioned regions of interest for functional characterization (indicated in Fig. 1B and Fig. S1C)—hypothesizing that these mutations would be actionable. Of the different mutants at the same position of ERBB4 amino acid sequence, the most recurrent amino acid change was selected for characterization.

To more comprehensively assess the recurrence of the selected *ERBB4* missense mutations (and the less frequent mutations at the same amino acid residue) in cancer patients, all such patient cases listed in three publicly available cancer registries (cBioPortal, AACR GENIE, and COSMIC) were combined and the nonoverlapping cases are shown in Fig. 1C. The numbers of patients ranged from 114 (R711/H/L/G/S mutations) to 20 (G907E/A/R/V mutations) (Fig. 1C).

3.2. Majority of the recurrent ERBB4 mutations are transforming in Ba/F3 or MCF10a cells

To study the functional significance of the 18 selected recurrent *ERBB4* mutations, we set out to screen their

Fig. 1. Cancer-associated *ERBB4* mutations selected for functional characterization. (A) Left and middle: fractions of *ERBB4* alterations in clinical cancer samples reported in cBioPortal (cbioportal.org) curated non-redundant studies (January 2024). Right: fractions of putative driver cases and variants of unknown significance (VUS) cases in all *ERBB4* missense mutated cancer samples (based on OncoKB curated evidence on putative oncogenicity of a given alteration). Of the *ERBB4* missense mutations reported in cBioPortal ($n = 2117$), 9% were annotated as putative drivers, and 91% as variants of unknown significance (VUS). (B) Lollipop diagram depicting the number of missense mutations at the indicated ERBB4 amino acid residues reported in cBioPortal. Light green denotes VUS and dark green denotes putative driver mutations based on OncoKB annotations. Regions of interest (red rectangles) demonstrate (1) paralogous mutations to known activating mutations described for other oncogenic ERBB family members and/or (2) location at dimerization interface suggesting functional relevance. The 18 recurrent missense mutations chosen for analyses are indicated. (C) Lollipop diagram showing the number of patients with the selected *ERBB4* mutations, or less frequent mutations targeting the same amino acid, reported in cBioPortal, AACR GENIE (genie.cbioportal.org) and COSMIC (cancer.sanger.ac.uk) (redundant cases removed). The MutationMapper tool of cBioPortal was used to visualize the data.

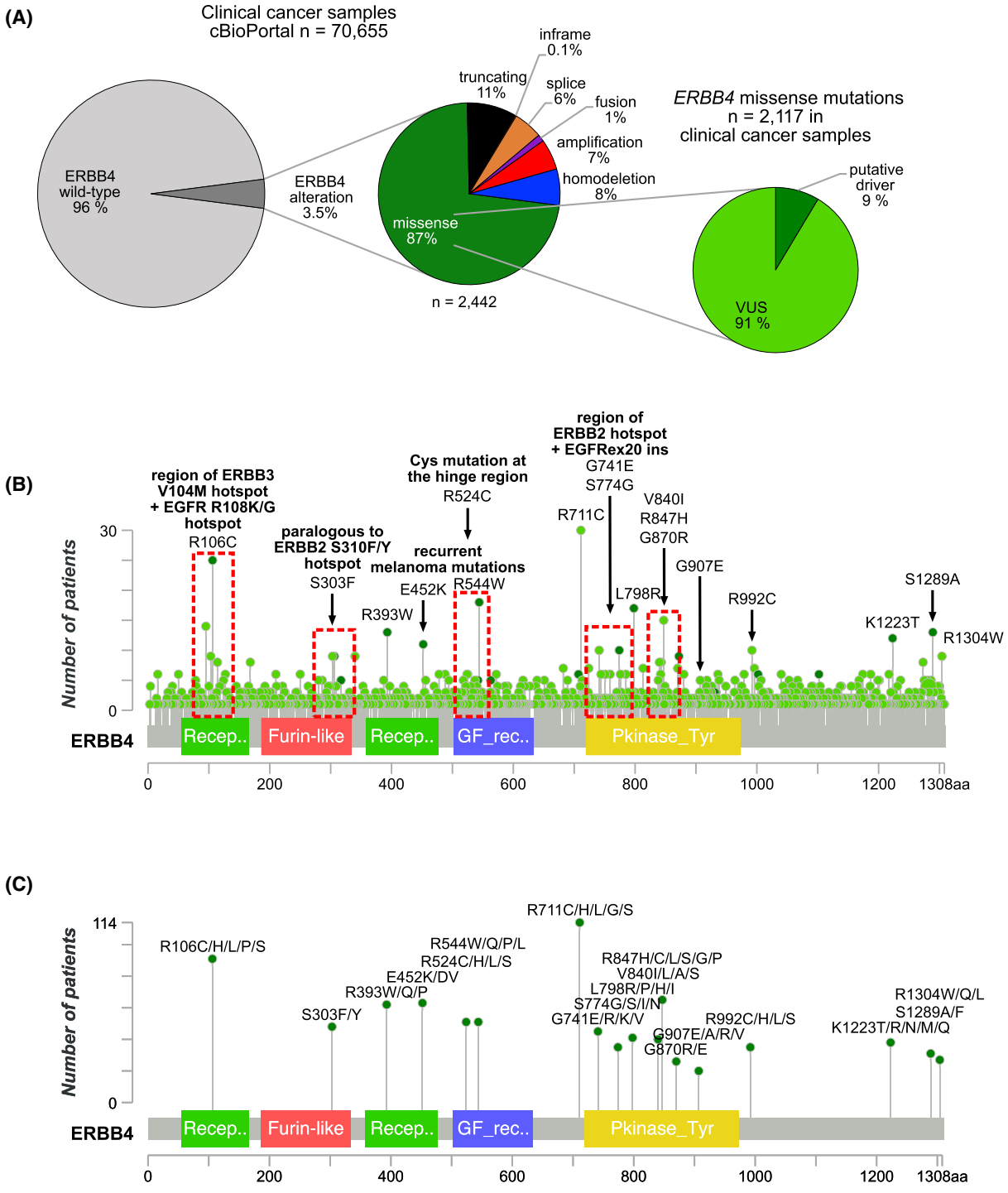

ability to transform (as outlined in Fig. 2A) two different nontumorigenic cell models: murine lymphoid Ba/F3 cells and human mammary epithelial MCF10a cells. Neither of these models express detectable levels of ERBB4. The ERBB4 JM-a CYT-2 isoform was used in the studies based on previous findings suggesting that JM-a CYT-2 is the more oncogenic ERBB4 isoform of the cancer-associated isoforms [23] in hematopoietic cell contexts (relevant for the Ba/F3 cell model) [6,22] and in numerous mammary epithelial cell contexts (relevant for the MCF10a cell model) [24,48–50]. Both the cell lines were retrovirally

transduced to stably express the selected ERBB4-mutants, wild-type ERBB4 or eGFP as a vector control (Fig. 2B). The different ERBB4− mutants demonstrated similar expression levels compared to wild-type ERBB4 in both model systems with the exception of R106C and G907E mutants that were expressed predominantly as immature receptor forms in both models, suggesting defective receptor maturation. Also, the R1304W mutant demonstrated lower expression levels in the Ba/F3 cells, and could not be expressed at all in the MCF10a cells (Fig. 2B). To assess the transforming potential of the ERBB4− mutants, cell proliferation was measured upon depriving Ba/F3 cells of exogenous IL3 or MCF10a cells of EGF, of which the proliferation of these cell lines is normally dependent on. The proliferation assays were conducted in the presence or absence of the ERBB4 ligand NRG-1 (10% serum). Eleven out of the 18 mutants were identified as significantly more transforming than wild-type ERBB4 in either of the two cell models, in the presence or absence of NRG-1, as summarized in a heatmap (Fig. 2C). Three of these mutants (S303F, E452K and L798R) demonstrated enhanced transforming activity in both cell models, implying context-independent transforming potential. Of note, wild-type ERBB4 was also capable of transforming both Ba/F3 and MCF10a cells in the presence but not in the absence of NRG-1 (Fig. 2D, E).

Remarkably, ERBB4 S303F was the only variant able to promote IL3-independent growth of Ba/F3 cells without NRG-1 (Fig. 2D). Five out of the 18 mutants (S303F, E452K, L798R, R992C, and S1289A) promoted IL3-independent Ba/F3 cell proliferation in the presence of NRG-1 more potently than wild-type ERBB4 ($q < 0.05$; Fig. 2D). In MCF10a cells, five mutants (S303F, R393W, E452K, R544W, and S774G) were more potent in promoting EGF-independent cell proliferation in the absence of NRG-1 than wild-type ERBB4 ($q < 0.05$; Fig. 2E). In the presence of NRG-1, six not completely overlapping mutants (S303F, E452K, R711C, L798R, V840I, and G870R) promoted MCF10a cell proliferation better than wild-type ERBB4 ($q < 0.05$; Fig. 2E).

Taken together, these analyses indicate a potential oncogenic role for 11 recurrent ERBB4 mutations. Eight of the mutations were transforming in only one of the models used, suggesting context-specificity. Three mutants (S303F, E452K, and L798R) were strongly transforming with the ability to transform both cell models, S303F being unique in its ability to transform both models in the absence of NRG-1.

3.3. Structural analysis of the transforming ERBB4 mutations

To study the mechanisms underlying the transforming potential of the three most potent ERBB4-mutants, their potential structural impact was assessed. The S303 residue of ERBB4 is located at the extracellular β-helical domain II (Fig. 3A) (in the sixth module out of seven small disulfide-containing modules [51]). In a monomeric structure of ERBB4 in the inactive tethered conformation, the side chain of S303 faces solvent and is hydrogen bonded to the side chain of T284 of module 5, whereas in a dimeric form the residue is in close proximity of the dimerization arm of the neighboring subunit (Fig. 3B). Two features of the S303F mutation would likely contribute to enhanced receptor activity. First, while the side chain of S303 is hydrophilic and faces the solvent in the tethered structure, the phenylalanine residue in the S303F-mutant prefers a hydrophobic environment. Second, in the active dimer S303F would be located within a hydrophobic pocket interacting with the side chains of L275 and Y268 (π–π stacking). This would likely result in ERBB4 S303F favoring the active, open conformation

Fig. 2. Recurrent *ERBB4* mutations have transforming potential. (A) Outline of the screen used to assess the transforming potential of 18 recurrent *ERBB4* mutations in non-tumorigenic Ba/F3 murine lymphoid cells and in MCF10a human mammary epithelial cells. Image created with BioRender.com. (B) Western analysis of ERBB4 expression in Ba/F3 and MCF10a cells lentivirally transduced to stably express the indicated ERBB4 variants and cultured in their respective standard complete media ($n = 2$). (C) Summary of the transforming activity of *ERBB4* mutations compared to wild-type *ERBB4*. Heatmap summarizes the data from D and E. ($n = 2$). X indicates a cell line that could not be generated despite several attempts. (D) The effect of ERBB4 variants on Ba/F3 cell doubling time upon IL3 deprivation in the presence or absence of 20 ng·mL^{-1} NRG-1 (10% serum). Cell proliferation was analyzed with MTT assay over time, and doubling times were calculated (Methods). Doubling times in the presence of NRG-1 were normalized to the average of wild-type ERBB4 expressing cells of each independent experiment ($n = 2$). (E) The effect of ERBB4 variants on MCF10a cell growth upon EGF deprivation in the presence or absence of 50 ng·mL^{-1} NRG-1 (10% serum). Cell proliferation was analyzed with the MTT assay on day 0 and 8 and fold changes in cell proliferation were calculated and normalized to the average of wild-type ERBB4 expressing cells of each independent experiment ($n = 2$). The dashed horizontal lines in D and E indicate the average of cells expressing wild-type ERBB4. Statistical significance in D and E was assessed by Kruskal–Wallis test, with *P*-values controlled for false discovery rate by two-stage linear step-up method of Benjamini, Krieger and Yekutieli. Asterisks indicate the *q*-values: *$q < 0.05$; **$q < 0.01$; $q < 0.001$. In (C), *q*-values from (D) and (E) are shown.

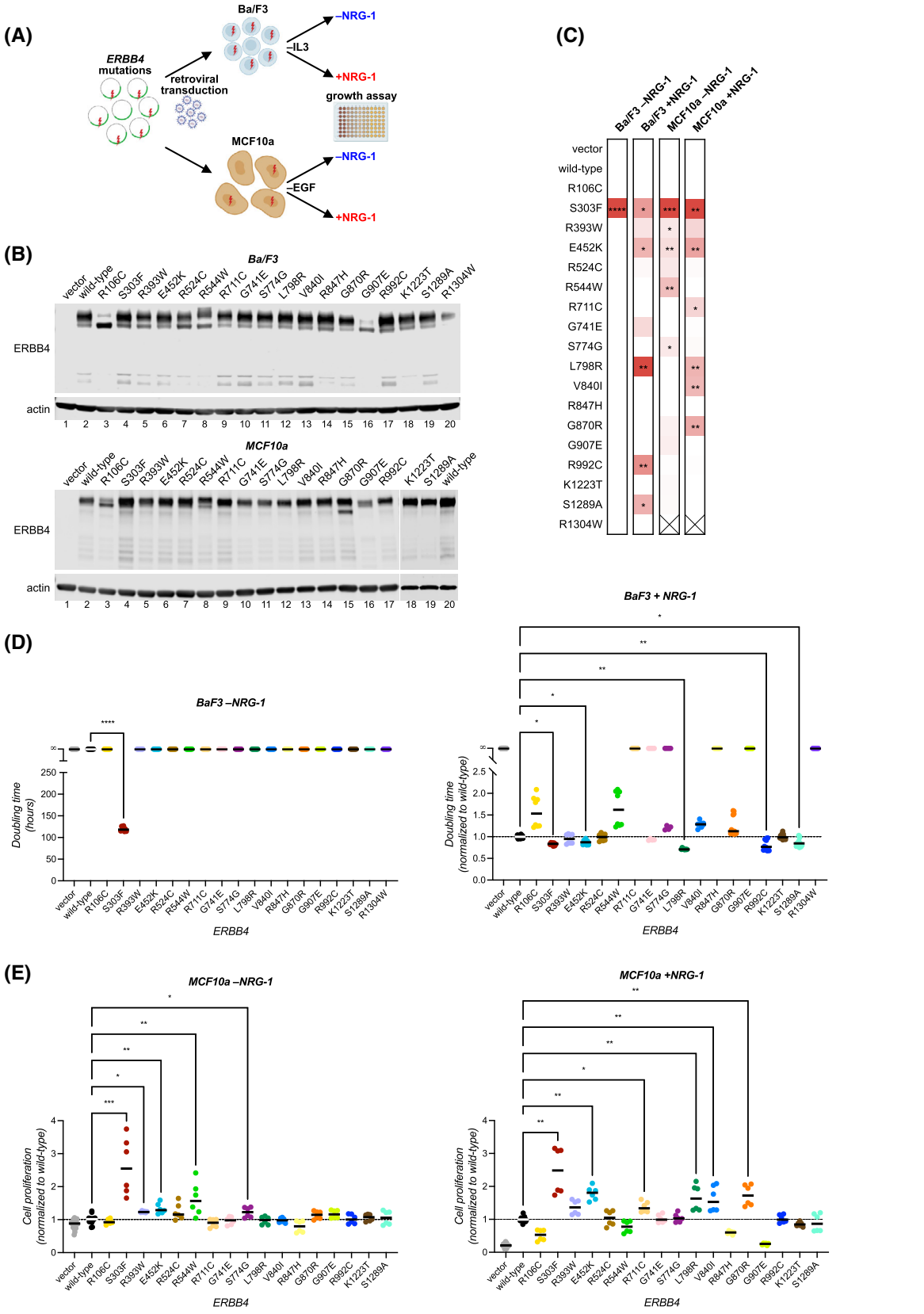

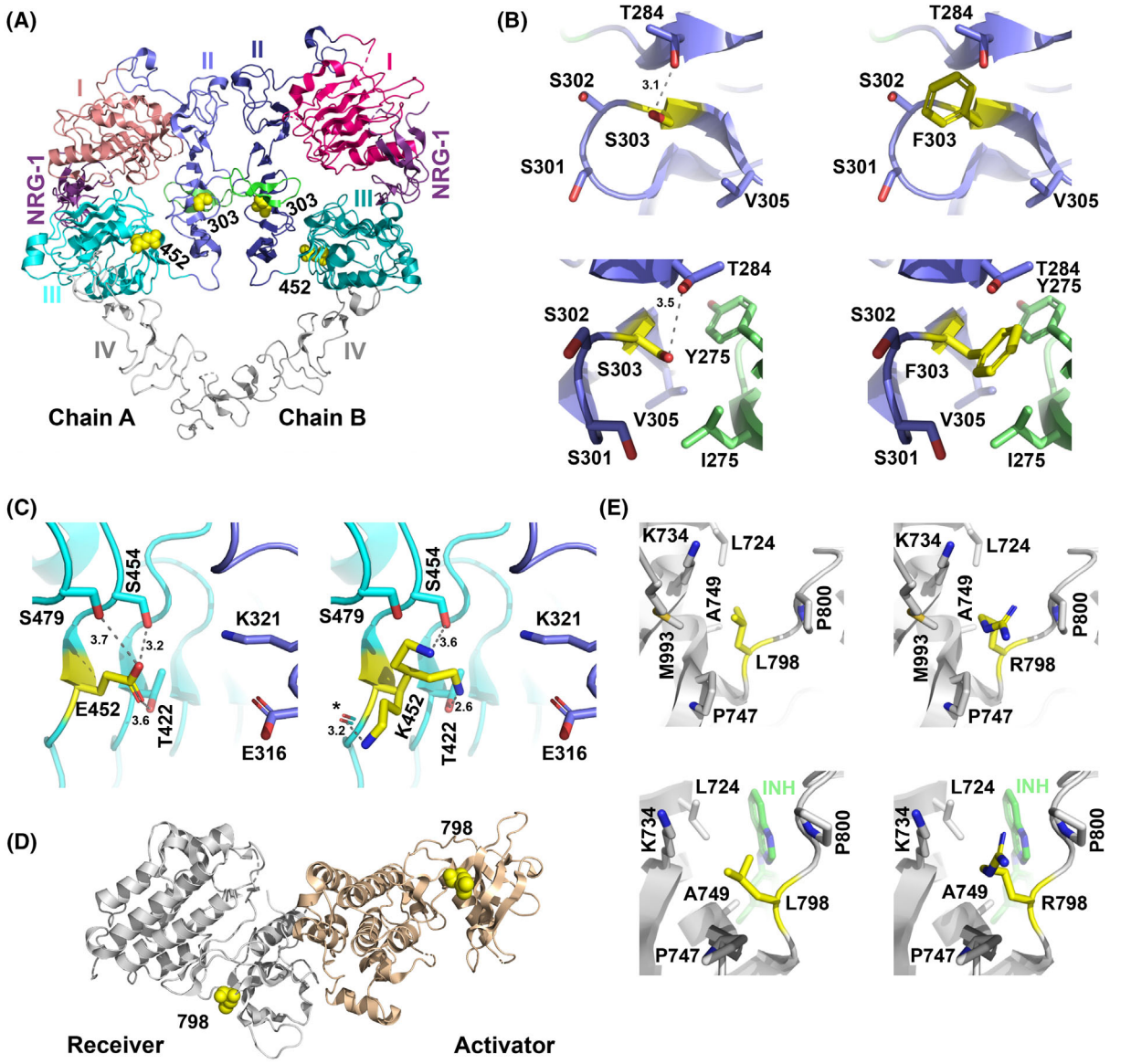

Fig. 3. Structural analysis of the S303F, E452K, and L798R mutations. (A) Structure of the ERBB4 extracellular domains in an NRG-1-bound active homodimer (PDB: 3U7U). Yellow spheres indicate the location of the S303F and E452K mutations. (B) The S303F mutation site, shown in the presence of S303 (left) or F303 (right). The upper and lower panels represent the tethered (PDB: 2AHX) and the active (PDB: 3U7U) conformations, respectively. (C) The E452K mutation site in the active dimer structure (PDB: 3U7U), shown in the presence of E452 (left) or K452 (right). Three potential lysine rotamers are shown. (D) The structure of the active ERBB4 asymmetric kinase dimer (PDB: 3BCE) with yellow spheres indicating the location of L798 in both the activator and receiver kinases. (E) The L798R mutation site, shown in the presence of L798 (left) or R798 (right). The upper and lower panels represent the active kinase in the asymmetric dimer (PDB: 3BCE) and the inactive kinase (PDB: 3BBT, inactive conformation with bound lapatinib (INH)), respectively.

over the inactive tethered conformation, and stabilizing interactions in the active dimer. The paralogous mutation S310F in ERBB2 was shown to stabilize a complex with ERBB3 and NRG-1 [52]. All in all, the mutation S310F is very likely to shift the equilibrium of ERBB4 monomers toward the active, extended dimeric state and directly foster receptor dimerization.

The E452K mutation is also extracellular and located at the interface of domains II and III (Fig. 3A). However, no direct contacts can be seen between these domains; a significant change in conformation would be needed for interdomain interactions, for example, with E316 and/or K321 of domain II (Fig. 3C). E452 seems to form a stable hydrogen-

bonding network with the surrounding residues T422, S454, and S479, whereas in the mutant, the lysine residue has multiple options to form hydrogen bonds, which may affect the dynamics of the interface and thereby foster indirectly dimer stability. In the tethered structure, E452 is facing the solvent and the mutation E452K is unlikely to cause any major effect in the equilibrium of the monomeric states.

Leucine 798 is positioned at the active site in the kinase domain (Fig. 3D) and within van der Waals interaction distance to the inhibitor (lapatinib) in the 3BBT structure (Fig. 3E, *lower panels*). In the active kinase domain structure of EGFR with bound ATP analog (PDB: 2GS6), an equivalent interaction between the paralogous leucine residue and an ATP analog exists. In the L798R-mutant, the bulky arginine residue may affect substrate binding at the active site and catalytic activity, for example, R798 could form π–π stacking interactions with the adenine ring of ATP leading to increased activity but this would require local conformational changes at the active site. However, it is not clear how the increased transformation potential caused by the L798R mutation affects the overall receptor structure or dimer stability.

3.4. Transforming ERBB4 mutations are activating and co-operate with other ERBB family members

To assess whether the three most potent ERBB4-mutants were transforming due to gain-of-function effect as proposed by the structural analyses, ERBB4 phosphorylation levels and downstream signaling pathway activation were analyzed in MCF10a cells (Fig. 4A). MCF10a cells express endogenously other ERBB family receptors, allowing heterodimerization with ERBB4, and thus, making MCF10a a relevant cellular context to study mutant ERBB4 signal transduction (Fig. 4A). Upon 8-day EGF deprivation (10% serum), corresponding to the conditions of the transformation assay (Fig. 2E), the strongly transforming ERBB4-mutants had indeed greater autophosphorylation levels both in the presence and absence of NRG-1. Additionally, EGFR, ERBB2, and ERBB3 were more phosphorylated in mutant ERBB4-expressing cells than in wild-type ERBB4-expressing or vector control cells in the presence and absence of NRG-1, most prominently in ERBB4 S303F-expressing cells (Fig. 4A, *lanes 5 and 6*). Consistently, the ERBB4 downstream signaling pathways were also more active in cells expressing ERBB4-mutants. In summary, these data indicate that S303F, E452K, and L798R are activating, gain-of-function ERBB4 mutations that may co-operate with other ERBB receptors in malignant transformation.

In contrast, when MCF10a cells were not subjected to 8-day EGF-deprivation but instead to short-term overnight serum starvation followed by NRG-1 stimulation for 10 min, there was no difference in ERBB4 phosphorylation between the transforming mutants and wild-type ERBB4 (Fig. S2A). Additionally, a gradual loss of wild-type ERBB4 but not ERBB4 S303F expression was observed over prolonged culture (≥ 10 weeks) of the stable MCF10a transductants (Fig. S2B,C) despite constant antibiotic selection to maintain the ERBB4-expressing pool of cells. The loss of wild-type ERBB4 occurred while maintaining the cells in the presence of EGF (Fig. S2B), suggesting that wild-type ERBB4 JM-a CYT-2, but not the S303F-mutant, provides selection disadvantage in the absence of transformation pressure. However, the EGF-independent growth of MCF10a cells mediated even by wild-type ERBB4 (Fig. 2E), together with the increased activation of the strongly transforming mutants observed upon EGF-deprivation (Fig. 4A) imply that ERBB4 activation favors the survival of breast epithelial cells upon deprived conditions providing selection pressure for transformed cells.

Since all three strongly transforming ERBB4-mutants, particularly ERBB4 S303F, promoted activation of all ERBB receptors in MCF10a cells (Fig. 4A), we hypothesized that ERBB4 heterodimerization might also be associated with cell transformation in Ba/F3 cells. Ba/F3 cells are known to endogenously express low levels of ERBB3 but no other ERBB receptors [53], and upregulation of endogenous ERBB3 expression is associated with Ba/F3 cell transformation promoted by other ERBB receptors, such as oncogenic mutants of EGFR (Fig. S3A). Indeed, ERBB4 S303F-transformed IL3-independent Ba/F3 cells had highly increased expression and phosphorylation levels of both ERBB4 and ERBB3 compared to nontransformed cells growing with IL3 (Fig. 4B). While ERBB4 S303F was more phosphorylated than wild-type ERBB4 at three different tyrosine residues (Y984, Y1162, Y1284) even in the presence of IL3, ERBB3 activation was only detectable in transformed, IL3-independent Ba/F3 cells.

To further investigate the role of ERBB3 upregulation in ERBB4-mediated Ba/F3 cell transformation, ERBB3 was knocked down in vector control cells and cells expressing ERBB4 wild-type or S303F using doxycycline-inducible murine *Erbb3* targeting shRNA (Fig. S3B). IL3-deprivation in the presence or absence of doxycycline revealed that *Erbb3* knockdown significantly impaired ERBB4 S303F-mediated, IL3-

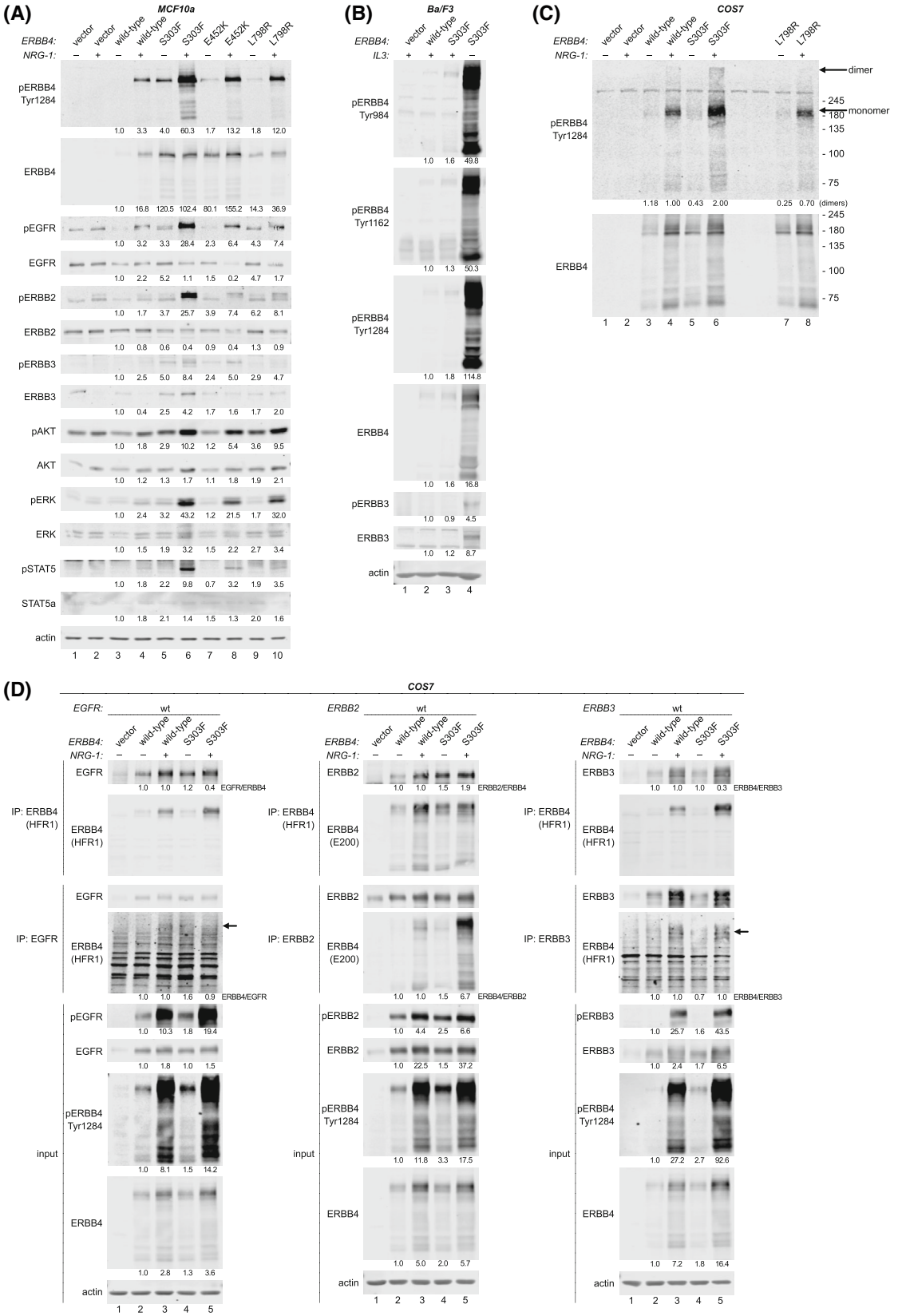

Fig. 4. Strongly transforming ERBB4 mutations are activating and co-operate with other ERBB receptors. (A) MCF10a cells stably expressing ERBB4 variants or vector control were cultured in the absence of EGF and in the absence or presence of 50 ng·mL^{-1} NRG-1 (10% serum) for 8 days. Lysates were analyzed by western blot using beta-Actin as a loading control ($n = 3$). (B) Ba/F3 cells stably expressing the indicated ERBB4 variants or vector control were cultured in the presence or absence of IL3 and analyzed by western blot ($n = 3$). (C) COS7 cells were transfected with constructs encoding ERBB4 variants or vector control and cultured in the absence of serum and in the presence or absence of 50 ng·mL^{-1} NRG-1 for 4 days. Cells were incubated with membrane impermeable BS_3 crosslinker and analyzed for phosphorylated ERBB4 dimers by western blot ($n = 2$). (D) COS7 cells co-transfected with an ERBB4 variant or vector control together with either EGFR, ERBB2 or ERBB3 were cultured as in (C). Cells were lysed and analyzed for heterodimerization by immunoprecipitation (IP) using either anti-ERBB4, anti-EGFR, anti-ERBB2 or anti-ERBB3 antibodies. IP samples and total lysates were analyzed by western blot using the indicated antibodies ($n = 2$). Densitometric quantification values below the blots indicate Actin-normalized fold changes to wild-type ERBB4 (−NRG) in A, B, and D (input). In C, values indicate phosphorylated dimer level fold changes to wild-type ERBB4 (+NRG-1) normalized to total ERBB4 levels. In IP blots, values indicate co-immunoprecipitation fold changes to wild-type ERBB4 (−NRG-1) normalized to the levels of the immunoprecipitated ERBB as indicated.

independent growth of Ba/F3 cells in the absence of NRG-1 (Fig. S3C,D, $P < 0.0001$). In contrast, *Erbb3* knockdown did not inhibit the growth of IL3-dependent cells, nor cells growing in the presence of NRG-1 (10% serum). Together, these data suggest that while ERBB4 can be transforming in the absence of other ERBB receptors, mutant ERBB4 co-operates with ERBB3 to promote ligand-independent cell transformation.

3.5. ERBB4 S303F stabilizes dimers

Considering the ability of ERBB4 S303F to broadly activate other ERBB receptors, and the structural analyses suggesting enhanced dimerization ability for ERBB4 S303F, we assessed the capability of ERBB4 S303F to form homodimers and heterodimers with other ERBB receptors. These experiments were performed with COS7 cells, which are devoid of endogenous ERBB4 and have low endogenous EGFR, ERBB2, and ERBB3 levels [54]. Transient overexpression was achieved using the retroviral pBABE-vector, which produces moderate protein expression levels in COS7 cells (Fig. S4A). Although ERBB4 S303F-mutant was slightly more phosphorylated after overnight serum starvation and 10-min NRG-1 stimulation than wild-type ERBB4 in COS7 cells (Fig. S4B, *Lanes 3 and 5*), the difference in ERBB4 phosphorylation between S303F and wild-type amplified over time in serum starvation (Fig. S4C). This is consistent with the observations of more prominently elevated phosphorylation levels of mutant ERBB4 compared to wild-type ERBB4 upon prolonged growth signal deprivation in both MCF10a (upon EGF deprivation: Fig. 4A vs. Fig. S2A) and Ba/F3 cells (upon IL3 deprivation: Fig. 4B, *Lanes 3 vs. 4*).

We selected four-day serum starvation for further experiments, demonstrating robust difference in ERBB4 wild-type and S303F phosphorylation levels, similar to what was observed in MCF10a and Ba/F3 cells. ERBB4 homodimers were assessed by crosslinking cell surface proteins with a cell membrane impermeable BS_3, enabling detection of ERBB4 dimers as high molecular weight species of ERBB4 in western blot. As predicted by the structural analyses, S303F resulted in more abundant active, phosphorylated ERBB4 dimers than wild-type ERBB4 in the presence of NRG-1, while the activating intracellular domain mutation L798R, that served as a negative control for dimer stabilization, did not (Fig. 4C).

To study the capability of ERBB4 S303F to form ERBB heterodimers, wild-type EGFR, ERBB2 or ERBB3 was cotransfected with ERBB4 wild-type or S303F, and heterodimerization was analyzed by co-immunoprecipitation. Interestingly, the expression levels of transiently transfected ERBB4 and ERBB3 were greater in the cells serum-starved for 4 days in the presence of NRG-1 than in its absence (Fig. 4D), suggesting that high expression of ERBB4 and ERBB3 provides growth-advantage for cells under serum starvation. Taking into account these expression level differences, ERBB4 S303F did indeed co-immunoprecipitate more efficiently than wild-type ERBB4 with ERBB2 both in the presence or absence of NRG-1 (Fig. 4D), demonstrating that the S303F mutation promotes the formation of ERBB heterodimers. Surprisingly, no difference in co-immunoprecipitation with ERBB3 was seen between S303F-mutant and wild-type ERBB4, although the experiments in Ba/F3 cells (Fig. 4B) suggested functional role for ERBB3 heterodimerization upon ERBB4 S303F-mediated establishment of IL3-independence. However, the COS7 cells expressing the S303F-mutant demonstrated greater phosphorylation levels of both ERBB4 and ERBB3 as compared to the cells expressing wild-type ERBB4, suggesting that ERBB4 S303F together with ERBB3 promoted cell survival during the four-day serum starvation.

Taken together, this *in vitro* evidence is consistent with the structural predictions that ERBB4 S303F can mediate its activating functions by stabilizing homo-

and heterodimers with other ERBB receptors but also that the heterodimerization is likely cell/tissue context-dependent.

3.6. Clinical efficacy of single-agent pan-ERBB inhibitor neratinib in patients with ERBB4 mutations

Despite the recurrence of *ERBB4* mutations in cancer and the existence of clinically used pan-ERBB inhibitors that potently also block ERBB4 activity, there are very limited data about the clinical actionability of *ERBB4* mutations. However, the SUMMIT basket trial (clinicaltrials.gov identifier NCT01953926) assessing the efficacy of pan-ERBB inhibitor neratinib in patients with somatic *ERBB2*, *ERBB3*, or *ERBB4* mutations, included seven patients harboring *ERBB4* alterations. Four of the seven patients had an *ERBB4* mutation characterized in this study. Two of the three patients that were qualified for the SUMMIT trial due to a mutation in *ERBB4*, with no other qualifying mutations in ERBB family genes, had an *ERBB4* mutation characterized in this study to be transforming (R544W and V840I) (Table S2). Yet, neither of these patients, nor the patient with an ERBB4 VUS N465K, responded to neratinib and progressed under treatment (Table S2).

Additionally, four patients that were enrolled to SUMMIT due to a mutation in *ERBB2* had co-occurring *ERBB4* mutations or *ERBB4* amplification (Table S2), including two mutations characterized as transforming in this study: the strongly transforming L798R mutation and R711C that was transforming in MCF10a cells but not in Ba/F3 cells. The ERBB4 L798R-mutant patient harbored also another ERBB4 VUS, N138S, and did not respond to neratinib while the patient harboring ERBB4 R711C had stable disease as the best response. It is noteworthy, that all the four patients whose *ERBB4* mutation is transforming *in vitro* had a co-occurring *TP53* alteration, and *TP53* mutations were associated with lack of response to neratinib in the SUMMIT trial [55].

3.7. Activating ERBB4 mutations are sensitive to clinically available pan-ERBB inhibitors

Next, we set out to determine the sensitivity of the strongly transforming ERBB4-mutants (S303F, E452K, L798R) to neratinib and the two other clinically used second-generation pan-ERBB inhibitors that are known to inhibit ERBB4 at a low nanomolar range, afatinib and dacomitinib [3]. All the three ERBB4 mutations rendered NRG-1-dependent Ba/F3 cells similarly sensitive to neratinib, afatinib, and dacomitinib as wild-type ERBB4 (Fig. 5A,B; $P > 0.05$). Although the patient harboring ERBB4 L798R mutation did not respond to neratinib in the SUMMIT trial (Table S2), and L798R is located in the ATP-binding pocket where it could potentially interfere with the binding of TKIs (Fig. 3D,E), these *in vitro* data showed that L798R did not mediate resistance to neratinib, afatinib, or dacomitinib.

In addition, we analyzed the pan-ERBB inhibitor sensitivity of the three other transforming ERBB4-mutants detected in the SUMMIT trial patients who did not respond to neratinib (R544W, R711C, V840I). Cells expressing ERBB4 V840I were equally sensitive with wild-type ERBB4 to all the three pan-ERBB inhibitors (Fig. 5A,B; $P > 0.05$), whereas cells expressing the R544W-mutant were significantly more sensitive (neratinib $P = 0.025$, afatinib $P = 0.038$, and dacomitinib $P = 0.041$). Also, the cells expressing ERBB4 R711C trended toward being more sensitive to pan-ERBB inhibition than the cells expressing wild-type ERBB4 but the comparison reached statistical significance only with afatinib ($P = 0.047$). These *in vitro* findings demonstrate that the unresponsiveness of the patients harboring ERBB4 R544W, V840I, R711C and L798R mutations to neratinib in the SUMMIT trial cannot be attributed to these being *bona fide* resistance mutations to neratinib. Instead, these data suggest that all the analyzed transforming ERBB4 mutations are sensitive to clinically available second-generation pan-ERBB inhibitors.

3.8. Characteristics of patient tumors harboring transforming ERBB4 mutations

Analyses of the patient cases included in cBioPortal, AACR GENIE and COSMIC showed that all the three mutants were highly cancer type specific, S303F occurring mostly in breast cancer (69%, 25/36), E452K in melanoma (85%, 52/61), and L798R in cancers of the gastrointestinal tract (esophagogastric 47%, 15/32 and colorectal 32%, 10/32) (Fig. S5A,B). Next, we investigated the frequency of co-occurring ERBB alterations (Fig. S5C,D), considering the potential co-operation of heterodimers and recent studies showing that ERBB genes often harbor multiple weaker mutations *in cis*, that is, compound mutations, resulting in enhanced receptor activation and oncogenicity [56,57]. Notably, S303F mutation occurred as the single ERBB alteration in 84% of the cases, and thus, the patients had significantly less co-occurring ERBB alterations than patients with any *ERBB4* alteration ($P = 0.037$), consistent with our observations that S303F is a strongly activating mutation. In contrast, E452K had significantly more co-occurring ERBB alterations

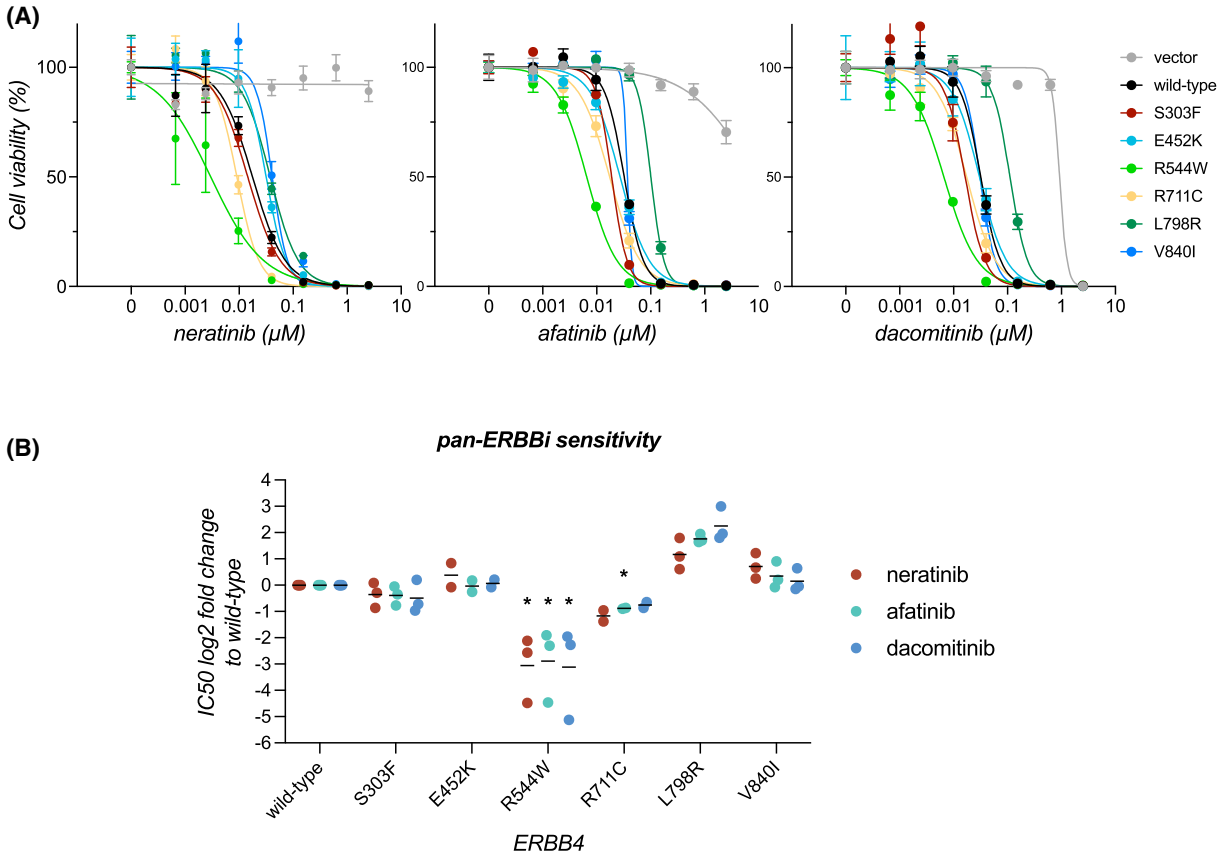

Fig. 5. Transforming ERBB4 mutants are sensitive to pan-ERBB inhibitors. (A) Sensitivity of Ba/F3 cells expressing different ERBB4 variants to pan-ERBB inhibitors. Ba/F3 cells expressing ERBB4 variants, growing in the absence of IL3 and presence of NRG-1 (10% serum), and vector control cells growing in the presence of IL3 were treated with the indicated concentrations of pan-ERBB inhibitors (neratinib, afatinib or dacomitinib) for 72 h and cell viability was measured with the MTT assay. A representative dose–response curve with mean and SD of quadruplicate analyses of one of independent experiments ($n = 3$ (E452K, R711C $n = 2$)) is shown for each inhibitor. (B) Fold changes in IC50 for Ba/F3 cells expressing ERBB4 variants, compared to Ba/F3 cells expressing wild-type ERBB4 are shown for each replicate experiment from A ($n = 3$ (E452K, R711C $n = 2$)). *$P < 0.05$; one-sample t test, P-values corrected for multiple comparisons by Bonferroni method. Horizontal lines indicate geometric means of the replicate experiments.

($P = 0.0005$), of which the majority were ERBB4 compound mutations, potentially indicative of co-operation of multiple weaker ERBB4 mutations. L798R, in turn, occurred as a single ERBB alteration in 65% of the cases, similar to clinical cancer samples with any *ERBB4* (64%), *EGFR* (62%) *ERBB2* (70%), or *ERBB3* (64%) alteration (Fig. S5D).

Taken together, these clinical sample data are in line with our *in vitro* results, suggesting that S303F is a potential driver mutation in breast cancer.

3.9. Activating ERBB4 mutations drive resistance to EGFR-targeted therapy in EGFR-mutant NSCLC cells

There is emerging evidence associating ERBB4 with cancer therapy resistance across various cancer types and treatment regimens [13,58–67], including *ERBB4* mutations that have been found in patient tumors after acquisition of therapy resistance [9–12,68]. Intriguingly, the *ERBB4* mutations identified in patients who developed resistance to EGFR-targeted therapy [10,12], include the same mutation or mutation in the same residue as analyzed in the current study: the strongly transforming S303F or L798I. In addition, while endogenous *ERBB4* mutations are rare in commercially available EGFR-mutant lung cancer cell lines, co-occurring *ERBB4* mutations have been found in EGFR-mutant lung cancer patients and have been shown to associate with shorter progression-free survival on EGFR inhibitor therapy [9]. These observations point to the possibility that mutant ERBB4 could promote resistance to targeted therapies. To address this, the effect of activating ERBB4 mutations

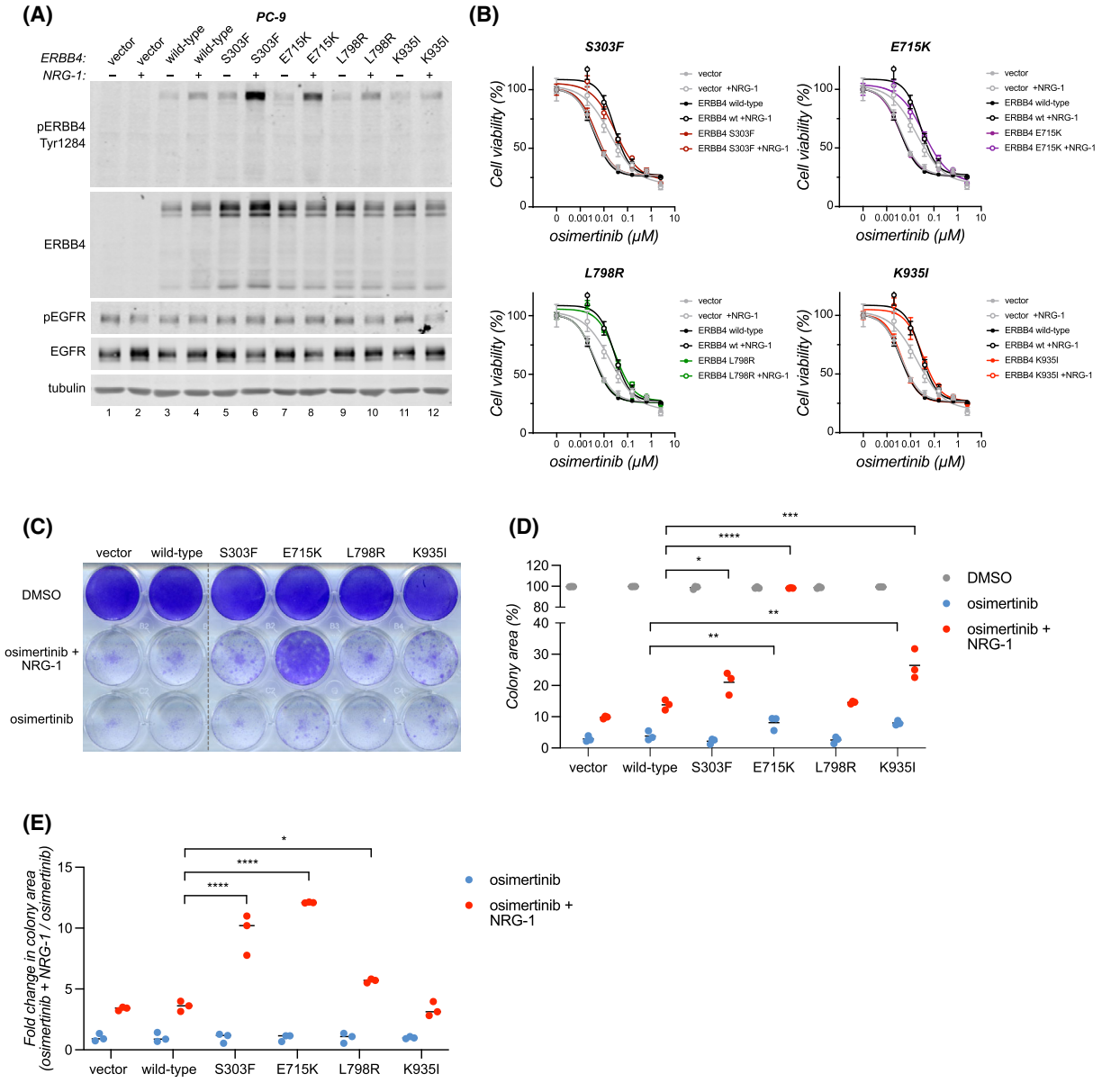

Fig. 6. Activating ERBB4 mutations drive resistance to EGFR-targeted therapy in EGFR-mutant NSCLC cells. (A) PC-9 cells stably expressing ERBB4 variants or vector control cells were serum-starved overnight and stimulated or not with 50 ng·mL^{-1} NRG-1 for 10 min. Lysates were analyzed by western using beta-tubulin as a loading control ($n = 2$). (B) PC-9 cells expressing ERBB4 variants were treated with the indicated concentrations of osimertinib in the presence or absence of 50 ng·mL^{-1} NRG-1 for 72 h (10% serum) and cell viability was measured with the MTT assay. The mean and SD of triplicate analyses of one of independent experiments ($n = 2$) are shown. (C) PC-9 cells were treated with 100 nM osimertinib for 14 days in the presence or absence of 50 ng·mL^{-1} NRG-1 (10% serum) and stained with crystal violet ($n = 3$). (D) Quantification of colony area data from C, shown as percentages of DMSO-treated controls ($n = 3$). (E) Colony area fold changes of NRG-1 and osimertinib-treated cells compared to osimertinib alone from the data shown in C and D ($n = 3$). *P*-values were calculated by one-way ANOVA with Šidák's multiple comparisons test in D and E. *$P < 0.05$; **$P < 0.01$; ***$P < 0.001$; ****$P < 0.0001$.

on EGFR inhibitor response in EGFR-mutant NSCLC cells was assessed. For this, we transduced PC-9 cells, lacking endogenous ERBB4, with wild-type ERBB4 or four activating ERBB4-mutants: S303F and L798I identified in this study, as well as previously identified E715K [6] and K935I [7]. Consistent with previous experiments (Fig. 4, [6,7]), the strongly activating S303F and E715K-mutants demonstrated increased ERBB4 activation compared to wild-type ERBB4 following short-term stimulation with NRG-1

after overnight serum starvation (Fig. 6A). On the other hand, the L798R and K935I-mutants did not exhibit enhanced ERBB4 activation, suggesting some context-dependency in mutant ERBB4 activation, at least in the steady-state setting. In short-term, three-day experiments, the mutant ERBB4-expressing PC-9 cells did not demonstrate any change in response to EGFR inhibitor osimertinib, either in the presence or absence of NRG-1 (10% serum) (Fig. 6B), when compared to wild-type ERBB4-expressing or vector control cells. It is noteworthy though that NRG-1 promoted a clear increase in osimertinib IC50 in all cell lines, indicating that NRG-1 (most likely through ERBB3) may affect EGFR inhibitor response.

In contrast to the short-term experiments, ERBB4-mutants S303F, E715K, and K935I significantly promoted resistance to osimertinib upon prolonged, 14-day treatment (10% serum) (Fig. 6C,D). All three mutants were able to confer osimertinib resistance in the presence of NRG-1, with the E715K-mutant demonstrating the most robust effect. The E715K and K935I-mutants were also able to promote osimertinib resistance in the absence of NRG-1, albeit quite weakly (Fig. 6C,D). These results are consistent with previous observations that activating, cancer-associated ERBB4 mutations typically enhance the ligand-mediated activation of ERBB4 (Fig. 4, [6,7]). Indeed, both S303F and E715K, as well as the L798R-mutant, demonstrated significantly increased responsiveness to NRG-1 under osimertinib treatment (Fig. 6E).

Together, these results demonstrate that activating ERBB4 mutations are able to confer resistance to EGFR-targeted therapy *in vitro*, and that this ability is particularly evident in the presence of an ERBB4 ligand.

3.10. Activating ERBB4 mutations promote resistance to EGFR-targeted therapy *in vivo*

In order to assess whether the activating ERBB4 mutations can also promote resistance to osimertinib *in vivo*, we subcutaneously implanted the PC-9 cells expressing wild-type ERBB4 or ERBB4-mutants S303F, E715K, L798R, and K935I in NMRI nude mice and analyzed the rate of relapse under continuous osimertinib treatment. While none of the PC-9 xenograft tumors expressing wild-type ERBB4 relapsed during the 189-day treatment, four out of 13 E715K tumors, three out of 12 S303F tumors, one out of 12 L798R tumors and one out of 13 K935I tumors relapsed during treatment. This translated to worse relapse-free survival under osimertinib for mice bearing ERBB4 E715K or S303F-expressing tumors (E715K, $P = 0.0398$; S303F, $P = 0.0826$) (Fig. 7A,B).

Considering the observations above that the ability of the ERBB4 S303F and E715K mutants to confer resistance to osimertinib is at least partly dependent on the availability of ERBB4 ligands (Fig. 6C–E), we analyzed the expression of ERBB4 ligands *in vivo* in PC-9 xenografts using previously published single-cell RNA-sequencing dataset [41]. As expected, the vehicle-treated and osimertinib-treated tumor cells clustered mostly separate in the UMAP space, indicating significant transcriptional changes in the tumor cells upon osimertinib treatment (Fig. 7C). The expression of ERBB4 ligands was significantly increased in the osimertinib-treated tumor cells compared to vehicle-treated cells, demonstrating that osimertinib treatment results in upregulation of ERBB4 ligand expression in PC-9 cells *in vivo* (Fig. 7C,D). Thus, it is plausible that this elevation in ERBB4 ligand expression provides the stimulus required for the ERBB4 mutants to promote resistance to osimertinib.

Together, these data provide compelling evidence that activating ERBB4 mutations can promote resistance to EGFR-targeted therapies *in vivo*.

4. Discussion

The high overall frequency of somatic *ERBB4* mutations in various cancer types and the existence of clinically approved pan-ERBB inhibitors that potently inhibit ERBB4 have raised the question whether *ERBB4*-mutant cancer patients could benefit from ERBB4-targeted therapy. Understanding the functional consequences of the mutations is indispensable for clinical decision making regarding targeted therapies [69]. Yet, unlike the frequent *ERBB2* amplifications in breast cancer and the activating kinase domain mutations of *EGFR* in lung cancer, mutations of *ERBB4*, *ERBB2*, and *ERBB3* are highly diverse across different cancer types, making it challenging to evaluate their clinical actionability. Especially *ERBB4* has lacked evident hotspot mutations although recurrent *ERBB4* mutations have started to emerge upon increased cancer profiling. While activating potential driver *ERBB4* mutations have been identified, these are rare in patients, which limits the possibility to clinically evaluate their potential to predict response to ERBB4-targeted therapy [4–7]. In addition, ERBB4 mutations have been detected in patients relapsing on EGFR-targeted therapies [9–12], potentially providing another context where ERBB4-targeting might be beneficial. Here, to better facilitate clinical interpretation of cancer-associated *ERBB4*

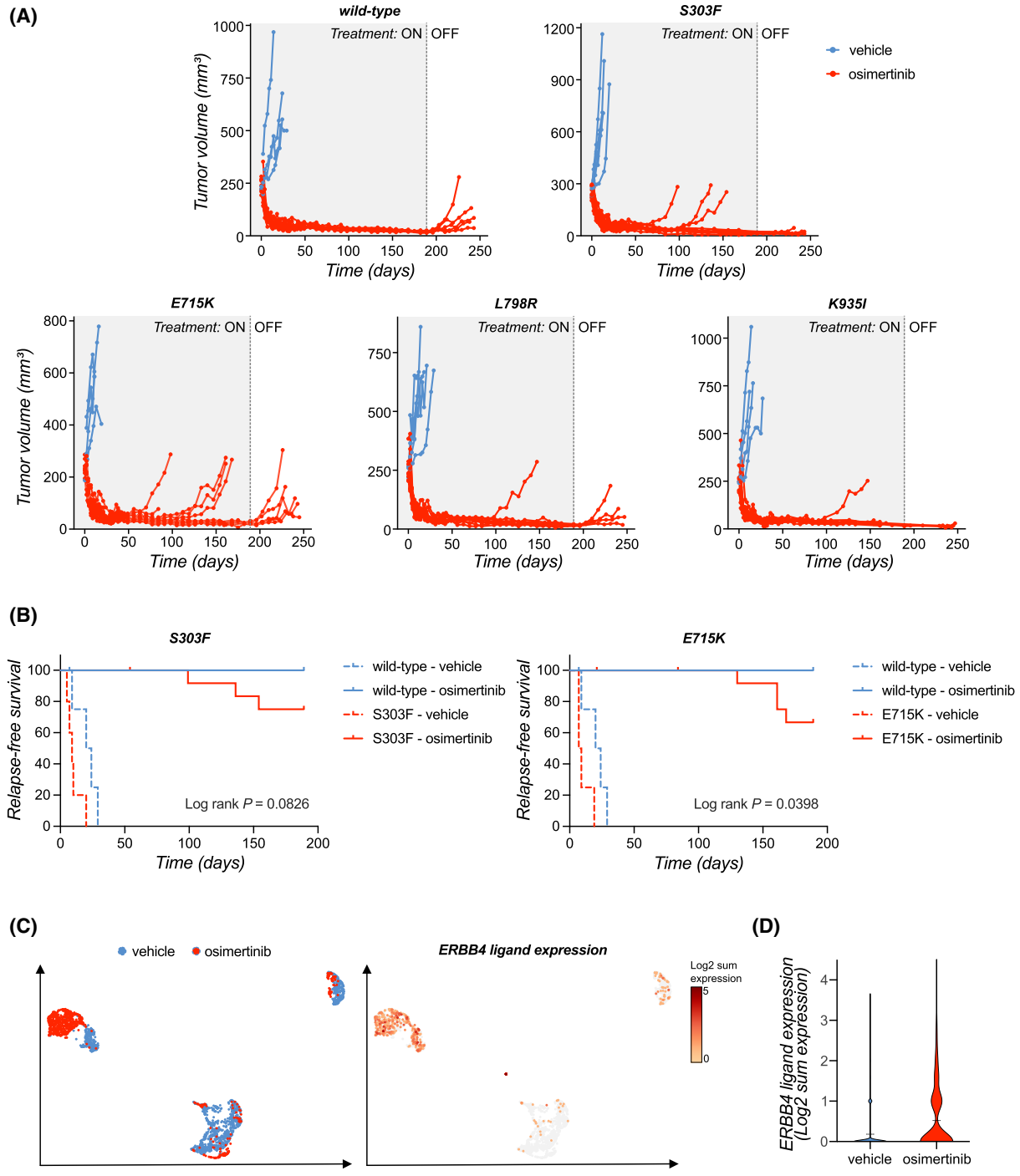

Fig. 7. Activating ERBB4 mutations promote resistance to EGFR-targeted therapy *in vivo*. (A) Tumor volumes of individual mice bearing xenograft tumors of PC-9 cells expressing ERBB4 variants and treated with vehicle ($n > 4$–5 per group) or osimertinib ($n > 11$–13 per group) for 189 days, followed by treatment withdrawal. (B) On-treatment relapse-free survival of mice treated with vehicle or osimertinib. Log rank test was used for the statistical analysis comparing the survival of mutant or wild-type ERBB4 xenograft-bearing mice under osimertinib treatment. (C) Single-cell RNA-sequencing analysis of ERBB4 ligand expression in PC-9 xenograft tumors from mice treated with vehicle or osimertinib for 21 days (GSE131604, [41]). Left: clustering of vehicle-treated (blue) and osimertinib-treated (red) tumor cells in the UMAP space. Right: ERBB4 ligand expression in tumor cells, shown as the log2 sum of *NRG1*, *NRG2*, *NRG3*, *NRG4*, *HBEGF*, *EREG* and *BTC* expression. (D) Violin plot of ERBB4 ligand expression in xenograft tumors from vehicle or osimertinib-treated mice.

mutations, we functionally characterized 18 recurrent *ERBB4* mutations.

Our results indicated that the majority of the analyzed *ERBB4* mutations (11/18) have oncogenic potential. While three of the mutants were strongly transforming in both nontumorigenic cell models, eight of the analyzed mutants were transforming in just one of the two cell models. Similar cell type-dependent transforming potential has been observed before with other oncogenic ERBB mutations. Strikingly, the most recurrent ERBB3 mutation V104M, known to be oncogenic and frequently occurring in gynecological and gastrointestinal tract cancers, is strongly transforming in MCF10a mammary epithelial cells and colon epithelial cells but not in Ba/F3 lymphoid cells [28,57]. Other examples of ERBB4 mutations with cell type-dependent transforming potential include E542K and G741R, as well as R544W that was also analyzed in this study using different cell models than previously [4,6]. The underlying causes for such cell type-dependent transforming potential are not fully understood but could be related to the mutant favoring certain dimerization partners or ligands for activating oncogenic signaling, and their different availability in a given cellular context. To overcome the limitations of focusing on a single cellular context, we used two very different cell models to address the transforming potential of ERBB4 variants: MCF10a cells that endogenously express EGFR, ERBB2, and ERBB3, and Ba/F3 cells that endogenously only express low levels of murine ERBB3. Neither of these models express detectable levels of ERBB4. It is possible that the remaining 7/18 mutants, not demonstrating significant transforming potential in this study, could be transforming in other cell types or tissue contexts.

Of the three mutants that were strongly transforming in both cell models, E452K has previously been shown to transform NIH-3T3 murine fibroblasts and to promote anchorage-independent growth of SK-MEL-2 human melanoma cells [4]. In contrast, the only previous functional study of ERBB4 S303F did not detect a growth promoting effect in an *ERBB2*-amplified breast cancer cell line HCC1569 [70]. This could be due to partial redundancy of the growth promoting functions of overactive ERBB2 and ERBB4.

Mechanistic analyses of the three most strongly transforming mutants (S303F, E452K, and L798R) showed that they were gain-of-function mutations enhancing the activity of other ERBB receptors and downstream signaling pathways, most prominently S303F. ERBB4 S303F was hyperphosphorylated even in the absence of a ligand, which reflected its ligand-independent transforming potential. Furthermore, our structural analyses proposed that the S303F mutation could result in stabilized dimer interactions (a) at the dimerization arm interface between the two monomers, and (b) destabilized interactions within a monomer favoring the active conformation. The dimerization assays confirmed that S303F-mutant ERBB4 formed more active homodimers and heterodimers with other ERBB receptors. The mechanism of activation is further supported by similar findings with the paralogous ERBB2 S310F mutation [52]. The ERBB2 S310F mutation makes the dimerization arm binding pocket of ERBB2 even more favorable for ERBB3 binding than the respective binding pockets in homodimers of wild-type EGFR or ERBB4, which in turn are considered the most stable ERBB dimers when bound to their high-affinity ligands [52,71,72]. This could perhaps also explain why ERBB4 S303F appears to enhance dimerization and activation of ERBB receptors even in the absence of a ligand.

The higher ERBB3 levels in Ba/F3 and MCF10a cells expressing ERBB4 S303F were indicative of enhanced ERBB3-ERBB4 co-operation, although ERBB4 S303F did not appear to dimerize more with ERBB3 than wild-type ERBB4 in the COS7 cell model. Indeed, knockdown of endogenous ERBB3 indicated that ERBB3 participated in ligand-independent, ERBB4 S303F-mediated transformation of Ba/F3 cells. While the moderate ERBB3 knockdown achieved in the experimental setup precluded definitive conclusions, ERBB3 knockdown did not seem to affect ERBB4-mediated Ba/F3 transformation in the presence of exogenous NRG-1. Moreover, the ERBB3 upregulation is also observed upon Ba/F3 cell transformation with well-established oncogenic mutants of EGFR (L858R, T790M) (Fig. S3A) and ERBB2 (S310F) [26]. This is in line with the recently recognized phenomenon of co-occurring ERBB mutations having synergistic effect on tumor growth and altering therapy sensitivity [56,73]. Together, these findings imply that ERBB4 heterodimers with other ERBB receptors can contribute to cell transformation and growth, supporting the rationale for pan-ERBB inhibition approach in targeting mutant ERBB4 in cancer.

Our *in vitro* results together strongly suggest that ERBB4 S303F, E452K, and L798R are potential driver mutations, especially S303F, which was found to occur usually as a sole ERBB alteration in cancer patient samples. We also showed that the three mutations were sensitive to clinically approved pan-ERBB inhibitors neratinib, afatinib, and dacomitinib, similar to several previously identified potential driver ERBB4 mutations [5–7,16]. Despite no clinical efficacy being observed in

the small cohort of seven *ERBB4*-mutant patients treated with neratinib in the SUMMIT trial, all four gain-of-function mutants found in SUMMIT trial patients were sensitive *in vitro* and thus not intrinsically resistant to neratinib. Unfortunately, the small number of *ERBB4* mutant patients does not allow the assessment of the genomic or cancer-type-related factors that were associated with a lack of response in *ERBB2*− mutant patients. For instance, the SUMMIT trial identified co-occurring *TP53* mutations to associate with a lack of response to neratinib in *ERBB2*-mutant patients [55]. Interestingly, all the patients with gain-of-function *ERBB4* mutations had a co-occurring *TP53* mutation. Additionally, three out of seven patients with *ERBB4* mutations also had co-occurring driver *ERBB2* mutations, which are known to be sensitive to neratinib in other cancer types but not in the cancer types that these patients had [55,74]. As an example, the strong ERBB2 driver mutation S310F is a hotspot in both breast cancer and bladder cancer but only breast cancer patients with the S310F mutation responded to neratinib [55]. We cannot exclude the possibility that such cancer type-specific responsiveness also extends to *ERBB4*-mutant tumors. It is also possible that the *ERBB4* alterations of the SUMMIT trial patients were not strong enough drivers, at least in these cancer types. Considering our strong evidence for ERBB4 S303F being a driver mutation and the high efficacy of neratinib in breast cancer, in which S303F appears most frequently, its potential as a predictive marker for neratinib should be clinically evaluated.

There is an increasing body of evidence from cell models, xenografts and patient data that ERBB4 can independently and together with ERBB3 (and/or with increased availability of their ligands) compensate for survival and growth signaling upon ERBB2- or EGFR-targeted therapy [13–17,60,75–77]. In addition, a recent study showed that *EGFR*-mutant lung cancer patients with co-occurring *ERBB4* mutations have shorter relapse-free survival on osimertinib treatment [9], further suggesting that *ERBB4* mutations may be associated with targeted therapy resistance in patients. Our results in the *EGFR*-mutant lung cancer context support this hypothesis, demonstrating that activating ERBB4 mutations are able to promote resistance to EGFR inhibitor osimertinib. Particularly, the S303F and the previously identified, strongly activating E715K mutation were able to confer resistance to osimertinib both *in vitro* and *in vivo*. While wild-type ERBB4 seems to be dispensable for steady-state proliferation for most cancer cell lines, it is intriguing to speculate that mutant ERBB4 activity may provide cancer cells with the means to survive stress associated with a lack of mitogenic signals, such as oncogene-targeted therapy. All the analyzed ERBB4 mutations demonstrated increased activity compared to wild-type ERBB4 upon prolonged serum starvation, and we have previously shown that activating ERBB4-mutants and ligand-stimulated wild-type ERBB4 promotes cell survival upon extended serum deprivation [6,7,21]. These findings point toward the importance of overactive ERBB4 in promoting survival of cancer cells, which aligns well with its role in promoting therapy resistance.

5. Conclusions

In conclusion, this study demonstrates that recurrent *ERBB4* mutations are potentially actionable in cancer rather than being inconsequential passenger mutations. In addition, we demonstrate that *ERBB4* mutations can promote resistance to targeted therapies. These data provide a rationale for further investigations into treating patients harboring activating *ERBB4* mutations with clinically available second-generation pan-ERBB inhibitors both in the treatment-naïve setting, as well as in the context of acquired targeted therapy resistance.

Acknowledgements

We thank Maria Tuominen and Mika Savisalo for skillful technical assistance, the bioinformatics (Jukka V. Lehtonen), drug discovery, and chemical biology and structural biology (FINStruct) infrastructure support from Biocenter Finland and CSC IT Center for Science for computational infrastructure support at the Structural Bioinformatics Laboratory, Åbo Akademi University, the NordForsk Nordic POP (Patient-Oriented Products), NordicPharmaTrain projects, and the Solutions for Health strategic area of Åbo Akademi University. The animal study was carried out with the support of Turku Center for Disease Modeling (TCDM), University of Turku, Finland; a member of Biocenter Finland. The authors would like to acknowledge the American Association for Cancer Research and its financial and material support in the development of the AACR Project GENIE registry, as well as members of the consortium for their commitment to data sharing. Interpretations are the responsibility of study authors. This study was supported by a research agreement with Puma Biotechnology (KE, KJK), as well as funding from the Research Council of Finland under grant numbers 346656 (KJK), 338466 (KJK), 316796 (KE), Sigrid Jusélius Foundation (KJK, KE, TTA, MSJ), Jane and Aatos Erkko Foundation (KJK), Finnish Cultural Foundation (KJK, VKO), Cancer Foundation Finland

(KE), Turku University Hospital (KE), InFLAMES Flagship Programme of the Research Council of Finland (decision number: 337531) (TTA, MSJ), the European Union – NextGenerationEU instrument and by the Research Council of Finland under grant number 352823 (TTA, MSJ), Cancer Society of South-West Finland (VKO), Instrumentarium Science Foundation (VKO), K. Albin Johansson Foundation (VKO), Orion Research Foundation (VKO), University of Turku Graduate School (VKO), and iCANDOC (The Finnish National Doctoral Education Pilot in Precision Cancer Medicine) at University of Turku (SP). Open access publishing facilitated by Turun yliopisto, as part of the Wiley - FinELib agreement.

Conflict of interest

This study was partly funded by a research agreement with Puma Biotechnology (KE, KJK).

Author contributions

VKO, KE, and KJK were involved in conceptualization. VKO, SA, SP, AT-K, OE, PS, AJ, IF, TTA, and MSJ were involved in investigation, data curation, and validation. VKO, SA, AT-K, OE, PS, DC, AJ, ND, TTA, MSJ, and KJK were involved in methodology. VKO, IF, TTA, MSJ, and KJK were involved in formal analysis. VKO, IF, TTA, MSJ, and KJK were involved in visualization. SB, LDE, and DC were involved in resources. VKO, DC, MSJ, KE, and KJK were involved in supervision. VKO, KE, and KJK were involved in project administration. VKO, TTA, MSJ, KE, and KJK were involved in funding acquisition. VKO, TTA, MSJ, and KJK were involved in writing – original draft. VKO, TTA, MSJ, LDE, KE, and KJK were involved in writing – review and editing.

Peer review

The peer review history for this article is available at https://www.webofscience.com/api/gateway/wos/peer-review/10.1002/1878-0261.70189.

Data accessibility

The data that support the findings of this study are available in Figs 1–7 and the Supporting Information of this article.

References

1 Arteaga CL, Engelman JA. ERBB receptors: from oncogene discovery to basic science to mechanism-based cancer therapeutics. *Cancer Cell*. 2014;**25**(3):282–303.
2 Yarden Y, Pines G. The ERBB network: at last, cancer therapy meets systems biology. *Nat Rev Cancer*. 2012;**12**:553–63.
3 Davis MI, Hunt JP, Herrgard S, Ciceri P, Wodicka LM, Pallares G, et al. Comprehensive analysis of kinase inhibitor selectivity. *Nat Biotechnol*. 2011;**29**(11):1046–51.
4 Prickett TD, Agrawal NS, Wei X, Yates KE, Lin JC, Wunderlich JR, et al. Analysis of the tyrosine kinome in melanoma reveals recurrent mutations in ERBB4. *Nat Genet*. 2009;**41**(10):1127–32.
5 Nakamura Y, Togashi Y, Nakahara H, Tomida S, Banno E, Terashima M, et al. Afatinib against esophageal or head-and-neck squamous cell carcinoma: significance of activating oncogenic HER4 mutations in HNSCC. *Mol Cancer Ther*. 2016;**15**(8):1988–97.
6 Chakroborty D, Ojala VK, Knittle AM, Drexler J, Tamirat MZ, Ruzicka R, et al. An unbiased functional genetics screen identifies rare activating ERBB4 mutations. *Cancer Res Commun*. 2022;**2**(1):10–27.
7 Kurppa KJ, Denessiouk K, Johnson MS, Elenius K. Activating ERBB4 mutations in non-small cell lung cancer. *Oncogene*. 2016;**35**(10):1283–91.
8 Tvorogov D, Sundvall M, Kurppa K, Hollmén M, Repo S, Johnson MS, et al. Somatic mutations of ErbB4: selective loss-of-function phenotype affecting signal transduction pathways in cancer. *J Biol Chem*. 2009;**284**(9):5582–91.
9 Vokes NI, Chambers E, Nguyen T, Coolidge A, Lydon CA, Le X, et al. Concurrent TP53 mutations facilitate resistance evolution in EGFR mutant lung adenocarcinoma. *J Thorac Oncol*. 2022;**17**(6):779–92.
10 Jänne PA, Baik C, Su WC, Johnson ML, Hayashi H, Nishio M, et al. Efficacy and safety of Patritumab Deruxtecan (HER3-DXd) in EGFR inhibitor– resistant, EGFR-mutated non–small cell lung cancer. *Cancer Discov*. 2022;**12**(1):74–89.
11 Yaeger R, Mezzadra R, Sinopoli J, Bian Y, Marasco M, Kaplun E, et al. Molecular characterization of acquired resistance to KRASG12C–EGFR inhibition in colorectal cancer. *Cancer Discov*. 2023;**13**(1):41–55.
12 Cremolini C, Benelli M, Fontana E, Pagani F, Rossini D, Fucà G, et al. Benefit from anti-EGFRs in RAS and BRAF wild-type metastatic transverse colon cancer: a clinical and molecular proof of concept study. *ESMO Open*. 2019;**4**(2):e000489.
13 Debets DO, Stecker KE, Piskopou A, Liefaard MC, Wesseling J, Sonke GS, et al. Deep (phospho) proteomics profiling of pre- treatment needle biopsies

identifies signatures of treatment resistance in HER2+ breast cancer. *Cell Rep Med*. 2023;**4**(10):101203.
14 Canfield K, Li J, Wilkins OM, Morrison MM, Ung M, Wells W, et al. Receptor tyrosine kinase ERBB4 mediates acquired resistance to ERBB2 inhibitors in breast cancer cells. *Cell Cycle*. 2015;**14**(4):648–55.
15 Shi J, Li F, Yao X, Mou T, Xu Z, Han Z, et al. The HER4-YAP1 axis promotes trastuzumab resistance in HER2-positive gastric cancer by inducing epithelial and mesenchymal transition. *Oncogene*. 2018;**37** (22):3022–38.
16 Donoghue JF, Kerr LT, Alexander NW, Greenall SA, Longano AB, Gottardo NG, et al. Activation of ERBB4 in glioblastoma can contribute to increased tumorigenicity and influence therapeutic response. *Cancers (Basel)*. 2018;**10**(8):243.
17 Carrión-Salip D, Panosa C, Menendez JA, Puig T, Oliveras G, Pandiella A, et al. Androgen-independent prostate cancer cells circumvent EGFR inhibition by overexpression of alternative HER receptors and ligands. *Int J Oncol*. 2012;**41**(3):1128–38.
18 Wali VB, Gilmore-Hebert M, Mamillapalli R, Haskins JW, Kurppa KJ, Elenius K, et al. Overexpression of ERBB4 JM-a CYT-1 and CYT-2 isoforms in transgenic mice reveals isoformspecific roles in mammary gland development and carcinogenesis. *Breast Cancer Res*. 2014;**16**(6):501.
19 Brockhoff G. "Shedding" light on HER4 signaling in normal and malignant breast tissues. *Cell Signal*. 2022;**97**:110401.
20 Lucas LM, Dwivedi V, Senfeld JI, Cullum RL, Mill CP, Piazza JT, et al. The yin and Yang of ERBB4: tumor suppressor and Oncoprotein. *Pharmacol Rev*. 2022;**74**(1):18–47.
21 Sundvall M, Veikkolainen V, Kurppa K, Salah Z, Tvorogov D, Joop Van Zoelen E, et al. Cell death or survival promoted by alternative isoforms of ErbB4. *Mol Biol Cell*. 2010;**21**:4275–86.
22 Määttä JA, Sundvall M, Junttila TT, Peri L, Laine VJO, Isola J, et al. Proteolytic cleavage and phosphorylation of a tumor-associated ErbB4 isoform promote ligand-independent survival and cancer cell growth. *Mol Biol Cell*. 2006;**17**(1):67–79.
23 Veikkolainen V, Vaparanta K, Halkilahti K, Iljin K, Sundvall M, Elenius K. Function of ERBB4 is determined by alternative splicing. *Cell Cycle*. 2011;**10** (16):2647–57.
24 Junttila TT, Sundvall M, Lundin M, Lundin J, Tanner M, Härkönen P, et al. Cleavable ErbB4 isoform in estrogen receptor–regulated growth of breast cancer cells. *Cancer Res*. 2005;**65**(4):1384–93.
25 Gilbertson R, Hernan R, Pietsch T, Pinto L, Scotting P, Allibone R, et al. Novel ERBB4 juxtamembrane splice variants are frequently expressed in childhood medulloblastoma. *Genes Chromosomes Cancer*. 2001;**31** (3):288–94.
26 Koivu MKA, Chakroborty D, Tamirat MZ, Johnson MS, Kurppa KJ, Elenius K. Identification of predictive ERBB mutations by leveraging publicly available cell line databases. *Mol Cancer Ther*. 2021;**20**(3):564–76.
27 Greulich H, Kaplan B, Mertins P, Chen TH, Tanaka KE, Yun CH, et al. Functional analysis of receptor tyrosine kinase mutations in lung cancer identifies oncogenic extracellular domain mutations of ERBB2. *Proc Natl Acad Sci U S A*. 2012;**109**(36):14476–81.
28 Jaiswal BSS, Kljavin NM, Stawiski EW, Chan E, Parikh C, Durinck S, et al. Oncogenic ERBB3 mutations in human cancers. *Cancer Cell*. 2013;**23** (5):603–17.
29 Chakroborty D, Kurppa KJ, Paatero I, Ojala VK, Koivu M, Tamirat MZ, et al. An unbiased *in vitro* screen for activating epidermal growth factor receptor mutations. *J Biol Chem*. 2019;**294**(24):9377–89.
30 Dull T, Zufferey R, Kelly M, Mandel RJ, Nguyen M, Trono D, et al. A third-generation lentivirus vector with a conditional packaging system. *J Virol*. 1998;**72** (11):8463–71.
31 Bouyain S, Longo PA, Li S, Ferguson KM, Leahy DJ. The extracellular region of ErbB4 adopts a tethered conformation in the absence of ligand. *Proc Natl Acad Sci U S A*. 2005;**102**(42):15024–9.
32 Liu P, Cleveland TE, Bouyain S, Byrne PO, Longo PA, Leahy DJ. A single ligand is sufficient to activate EGFR dimers. *Proc Natl Acad Sci U S A*. 2012;**109** (27):10861–6.
33 Qiu C, Tarrant MK, Choi SH, Sathyamurthy A, Bose R, Banjade S, et al. Mechanism of activation and inhibition of the HER4/ErbB4 kinase. *Structure*. 2008;**16**(3):460–7.
34 Wiederschain D, Wee S, Chen L, Loo A, Yang G, Huang A, et al. Single-vector inducible lentiviral RNAi system for oncology target validation. *Cell Cycle*. 2009;**8**(3):498–504.
35 Cerami E, Gao J, Dogrusoz U, Gross BE, Sumer SO, Aksoy BA, et al. The cBio cancer genomics portal: an open platform for exploring multidimensional cancer genomics data. *Cancer Discov*. 2012;**2**(5):401–4.
36 Gao J, Aksoy BA, Dogrusoz U, Dresdner G, Gross B, Sumer SO, et al. Integrative analysis of complex cancer genomics and clinical profiles using the cBioPortal. *Sci Signal*. 2013;**6**(269):pl1.
37 de Bruijn I, Kundra R, Mastrogiacomo B, Tran TN, Sikina L, Mazor T, et al. Analysis and visualization of longitudinal genomic and clinical data from the AACR project GENIE biopharma collaborative in cBioPortal. *Cancer Res*. 2023;**83**(23):3861–7.
38 Sweeney SM, Cerami E, Baras A, Pugh TJ, Schultz N, Stricker T, et al. AACR project GENIE: powering

precision medicine through an international consortium. *Cancer Discov*. 2017;**7**(8):818–31.
39 Forbes SA, Beare D, Boutselakis H, Bamford S, Bindal N, Tate J, et al. COSMIC: somatic cancer genetics at high-resolution. *Nucleic Acids Res*. 2017;**45**(D1):D777–83.
40 Schneider CA, Rasband WS, Eliceiri KW. NIH Image to ImageJ: 25 years of image analysis. *Nat Methods*. 2012;**9**(7):671–5.
41 Kurppa KJ, Liu Y, To C, Zhang T, Fan M, Vajdi A, et al. Treatment-induced tumor dormancy through YAP-mediated transcriptional reprogramming of the apoptotic pathway. *Cancer Cell*. 2020;**37**(1):104–122.e12.
42 Chakravarty D, Gao J, Phillips SM, Kundra R, Zhang H, Wang J, et al. OncoKB: a precision oncology Knowledge Base. *JCO Precis Oncol*. 2017;**2017**: PO.17.00011.
43 Suehnholz SP, Nissan MH, Zhang H, Kundra R, Nandakumar S, Lu C, et al. Quantifying the expanding landscape of clinical Actionability for patients with cancer. *Cancer Discov*. 2024;**14**(1):49–65.
44 Lee JC, Vivanco I, Beroukhim R, Huang JHY, Feng WL, Debiasi RM, et al. Epidermal growth factor receptor activation in glioblastoma through novel missense mutations in the extracellular domain. *PLoS Med*. 2006;**3**(12):e485.
45 Bose R, Kavuri SM, Searleman AC, Shen W, Shen D, Koboldt DC, et al. Activating HER2 mutations in HER2 gene amplification negative breast cancer. *Cancer Discov*. 2013;**3**(2):224–37.
46 Greulich H, Chen TH, Feng W, Jänne PA, Alvarez JV, Zappaterra M, et al. Oncogenic transformation by inhibitor-sensitive and -resistant EGFR mutants. *PLoS Med*. 2005;**2**(11):e313.
47 Ferguson KM, Berger MB, Mendrola JM, Cho HS, Leahy DJ, Lemmon MA. EGF activates its receptor by removing interactions that autoinhibit Ectodomain dimerization. *Mol Cell*. 2003;**11**(2):507–17.
48 Muraoka-Cook RS, Sandahl MA, Strunk KE, Miraglia LC, Husted C, Hunter DM, et al. ErbB4 splice variants Cyt1 and Cyt2 differ by 16 amino acids and exert opposing effects on the mammary epithelium in vivo. *Mol Cell Biol*. 2009;**29**(18):4935–48.
49 Sartor CI, Zhou H, Kozlowska E, Guttridge K, Kawata E, Caskey L, et al. HER4 mediates ligand-dependent Antiproliferative and differentiation responses in human breast cancer cells. *Mol Cell Biol*. 2001;**21**(13):4265–75.
50 Vidal GA, Clark DE, Marrero L, Jones FE. A constitutively active ERBB4/HER4 allele with enhanced transcriptional coactivation and cell-killing activities. *Oncogene*. 2007;**26**(3):462–6.
51 Cho HS, Leahy DJ. Structure of the extracellular region of HER3 reveals an Interdomain tether. *Science*. 2002;**297**(5585):1330–3.
52 Diwanji D, Trenker R, Thaker TM, Wang F, Agard DA, Verba KA, et al. Structures of the HER2–HER3–NRG1β complex reveal a dynamic dimer interface. *Nature*. 2021;**600**(7888):339–43.
53 Riese DJ, van Raaij TM, Plowman GD, Andrews GC, Stern DF. The cellular response to neuregulins is governed by complex interactions of the erbB receptor family. *Mol Cell Biol*. 1995;**15**(10):5770–6.
54 Sawano A, Takayama S, Matsuda M, Miyawaki A. Lateral propagation of EGF signaling after local stimulation is dependent on receptor density. *Dev Cell*. 2002;**3**(2):245–57.
55 Hyman DM, Piha-Paul SA, Won H, Rodon J, Saura C, Shapiro GI, et al. HER kinase inhibition in patients with HER2-and HER3-mutant cancers. *Nature*. 2018;**554**(7691):189–94.
56 Saito Y, Koya J, Araki M, Kogure Y, Shingaki S, Tabata M, et al. Landscape and function of multiple mutations within individual oncogenes. *Nature*. 2020;**582**(7810):95–9.
57 Koivu MKA, Chakroborty D, Airenne TT, Johnson MS, Kurppa KJ, Elenius K. Trans-activating mutations of the pseudokinase ERBB3. *Oncogene*. 2024;**43**(29):2253–65.
58 Wang DS, Liu ZX, Lu YX, Bao H, Wu X, Zeng ZL, et al. Liquid biopsies to track trastuzumab resistance in metastatic HER2-positive gastric cancer. *Gut*. 2019;**68**(7):1152–61.
59 Zhang J, Qiu W, Zhang W, Chen Y, Shen H, Zhu H, et al. Tracking of trastuzumab resistance in patients with HER2-positive metastatic gastric cancer by CTC liquid biopsy. *Am J Cancer Res*. 2023;**13**(11):5684–97.
60 Nafi SNM, Generali D, Kramer-Marek G, Gijsen M, Strina C, Cappelletti M, et al. Nuclear HER4 mediates acquired resistance to trastuzumab and is associated with poor outcome in HER2 positive breast cancer. *Oncotarget*. 2014;**5**(15):5934–49.
61 Arribas AJ, Napoli S, Cascione L, Barnabei L, Sartori G, Cannas E, et al. ERBB4-mediated signaling is a mediator of resistance to BTK and PI3K inhibitors in B cell lymphoid neoplasms. *Mol Cancer Ther*. 2024;**23**(3):368–80.
62 Wege AK, Chittka D, Buchholz S, Klinkhammer-Schalke M, Diermeier-Daucher S, Zeman F, et al. HER4 expression in estrogen receptor-positive breast cancer is associated with decreased sensitivity to tamoxifen treatment and reduced overall survival of postmenopausal women. *Breast Cancer Res*. 2018;**20**(1):139.
63 Albert V, Bruss C, Tümen D, Piendl G, Weber F, Dahl E, et al. HER4 affects sensitivity to tamoxifen and Abemaciclib in luminal breast cancer cells and restricts tumor growth in MCF-7-based humanized tumor mice. *Int J Mol Sci*. 2024;**25**(13):7475.
64 Saglam O, Xiong Y, Marchion DC, Strosberg C, Wenham RM, Johnson JJ, et al. ERBB4 expression in

ovarian serous carcinoma resistant to platinum-based therapy. *Cancer Control*. 2017;**24**(1):89–95.
65 Merimsky O, Issakov J, Bickels J, Kollender Y, Flusser G, Soyfer V, et al. ErbB-4 expression in limb soft-tissue sarcoma: correlation with the results of neoadjuvant chemotherapy. *Eur J Cancer*. 2002;**38**(10):1335–42.
66 Mendoza-Naranjo A, El-Naggar A, Wai DH, Mistry P, Lazic N, Ayala FRR, et al. ERBB4 confers metastatic capacity in Ewing sarcoma. *EMBO Mol Med*. 2013;**5**(7):1019–34.
67 Merimsky O, Staroselsky A, Inbar M, Schwartz Y, Wigler N, Mann A, et al. Correlation between c-erbB-4 receptor expression and response to gemcitabine-cisplatin chemotherapy in non-small-cell lung cancer. *Ann Oncol*. 2001;**12**(8):1127–31.
68 Yuan SQ, Nie RC, Huang YS, Chen YB, Wang SY, Sun XW, et al. Residual circulating tumor DNA after adjuvant chemotherapy effectively predicts recurrence of stage II-III gastric cancer. *Cancer Commun*. 2023;**43**(12):1312–25.
69 Hyman DM, Taylor BS, Baselga J. Implementing genome-driven oncology. *Cell*. 2017;**168**:584–99.
70 Elster N, Toomey S, Fan Y, Cremona M, Morgan C, Weiner Gorzel K, et al. Frequency, impact and a preclinical study of novel ERBB gene family mutations in HER2-positive breast cancer. *Ther Adv Med Oncol*. 2018;**10**:1–16.
71 Bai X, Sun P, Wang X, Long C, Liao S, Dang S, et al. Structure and dynamics of the EGFR/HER2 heterodimer. *Cell Discov*. 2023;**9**(1):18.
72 Trenker R, Diwanji D, Bingham T, Verba KA, Jura N. Structural dynamics of the active HER4 and HER2/HER4 complexes is finely tuned by different growth factors and glycosylation. *Elife*. 2024;**12**:RP92873.
73 Hanker AB, Brown BP, Meiler J, Marín A, Jayanthan HS, Ye D, et al. Co-occurring gain-of-function mutations in HER2 and HER3 modulate HER2/HER3 activation, oncogenesis, and HER2 inhibitor sensitivity. *Cancer Cell*. 2021;**39**(8):1099–1114.e8.
74 Chan A, Delaloge S, Holmes FA, Moy B, Iwata H, Harvey VJ, et al. Neratinib after trastuzumab-based adjuvant therapy in patients with HER2-positive breast cancer (ExteNET): a multicentre, randomised, double-blind, placebo-controlled, phase 3 trial. *Lancet Oncol*. 2016;**17**(3):367–77.
75 Wilson TR, Fridlyand J, Yan Y, Penuel E, Burton L, Chan E, et al. Widespread potential for growth-factor-driven resistance to anticancer kinase inhibitors. *Nature*. 2012;**487**(7408):505–9.
76 Yonesaka K, Kudo K, Nishida S, Takahama T, Iwasa T, Yoshida T, et al. The pan-HER family tyrosine kinase inhibitor afatinib overcomes HER3 ligand heregulin-mediated resistance to EGFR inhibitors in non-small cell lung cancer. *Oncotarget*. 2015;**6**(32):33602–11.
77 Udagawa H, Nilsson MB, Robichaux JP, He J, Poteete A, Jiang H, et al. HER4 and EGFR activate cell signaling in NRG1 fusion-driven cancers: implications for HER2-HER3-specific versus pan-HER targeting strategies. *J Thorac Oncol*. 2023;**19**(1):106–18.

Supporting information

Additional supporting information may be found online in the Supporting Information section at the end of the article.

Fig. S1. ERBB4 alterations in clinical cancer samples.

Fig. S2. Biochemical activity and expression of ERBB4 variants in MCF10a cells in the absence of transformation pressure.

Fig. S3. Role of ERBB3 in ERBB4-mediated transformation of Ba/F3 cells.

Fig. S4. Effect of prolonged serum starvation on ERBB4 wild-type and S303F mutant activity in COS7 cells.

Fig. S5. Tumor characteristics of patients harboring somatic transforming ERBB4 mutations.

Table S1. Expression plasmids generated in this work.

Table S2. Patients harboring *ERBB4* alterations and treated with neratinib in the SUMMIT trial.